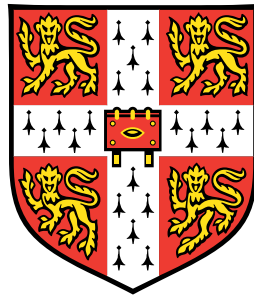


# Thermal Energy Recovery in Domestic Ovens

Part IIB Research Project



University of Cambridge

Department of Chemical Engineering and Biotechnology

Cody Kwok

Churchill College

Supervised by Jamie Davidson, Mark Williamson, Ian Wilson

## Preface

The work described in this report is the result of my own research, unaided except as specifically acknowledged in the text, and does not contain material that has already been used to any substantial extent for a comparable purpose. This report contains 40 pages and 9944 words (excluding the title page, this page and the safety appendix).

Signed by student



Date:

6th May 2022

I confirm that I have cleared the laboratory space I have used for the work described in this report, to the satisfaction of my project supervisor and the responsible laboratory technician. All chemical and biological samples have been properly and safely disposed of according to University guidance.

Signed by student

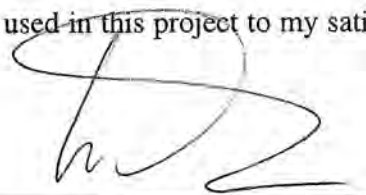


Date:

6th May 2022

I confirm that the student above has cleared the laboratory space used in this project to my satisfaction.

Signed by Project Supervisor



Date:

6th May 2022

Signed by Responsible Laboratory Technician



Date:

6th May 2022

## Summary

Since domestic ovens are one of the least energy efficient kitchen appliances, there is a clear impetus within companies to produce more energy efficient ovens, especially as electricity prices have gone up continuously and electricity production still accounts for a quarter of global greenhouse gas emissions. Cambridge Sensor Innovation has recently created a cooler unit to reduce the emission of volatile oils and fats from the oven cavity into the kitchen which can cause greasy films on surfaces. As vented gases from the oven pass through the cooler unit, they transfer their thermal energy into water within, simultaneously removing volatile lipids by condensation. The cooler unit also has the potential to recover energy through heating the water within; however, these energy savings can only be realised if this water is subsequently used (*e.g.* for household chores).

In this project, the cooler unit was commissioned and connected to an outlet made at the back of a standard 'true' electric fan convection oven. A thermal and electrical energy monitoring system was installed and commissioned on both items. Experiments were performed at set point temperatures of 160°C, 200°C and 240°C and a model food piece which released water into the oven cavity was used to test the system. The heat transfer performance of the oven was quantified and major sources of heat loss were identified. The highest temperature reached by the air leaving the cooler unit was 30°C, which is lower than the dew points of lipid-water vapour mixtures emitted by common food items during cooking. Additionally, heat transfer was not rate limited as it was dominated by forced convection, indicating that the cooler unit could theoretically condense these volatile lipids out of the vented gases. During 'normal' operation without any modifications to a standard oven, a total oven efficiency (the proportion of energy consumed by the oven which is either used for 'cooking' or is recovered) of 15.6 – 17.2% was obtained. With the cooler unit attached, an additional 1.0% of the energy consumed by the oven was recovered, improving the total oven efficiency to 16.6 – 18.2%.

# Contents

|                                                         |           |
|---------------------------------------------------------|-----------|
| <b>Summary</b>                                          | <b>1</b>  |
| <b>1 Introduction and Background</b>                    | <b>3</b>  |
| 1.1 Domestic Ovens . . . . .                            | 3         |
| 1.2 Motivation . . . . .                                | 4         |
| 1.3 Project Aims . . . . .                              | 6         |
| <b>2 Experimental Methods</b>                           | <b>7</b>  |
| 2.1 Apparatuses . . . . .                               | 7         |
| 2.1.1 Oven Unit . . . . .                               | 7         |
| 2.1.2 Cambridge Sensor Innovation Cooler Unit . . . . . | 8         |
| 2.1.3 Oven-Cooler Unit Connection . . . . .             | 9         |
| 2.2 Measurements . . . . .                              | 9         |
| 2.2.1 Temperature and Power . . . . .                   | 9         |
| 2.2.2 Air Flowrate . . . . .                            | 10        |
| 2.3 Main Experimental Campaigns . . . . .               | 11        |
| <b>3 Calculations</b>                                   | <b>14</b> |
| 3.1 Heat Transfer Coefficients . . . . .                | 14        |
| 3.2 Air Flowrates . . . . .                             | 16        |
| 3.3 Energy Balances . . . . .                           | 16        |
| 3.4 Efficiencies . . . . .                              | 20        |
| 3.5 Cooler Unit Heat Exchanger Models . . . . .         | 20        |
| <b>4 Results and Discussion</b>                         | <b>21</b> |
| 4.1 Phase 1 . . . . .                                   | 21        |
| 4.2 Phase 2 . . . . .                                   | 24        |
| 4.3 Phase 3 . . . . .                                   | 26        |
| 4.4 Phase 4 . . . . .                                   | 28        |
| 4.5 Proposals for Further Work . . . . .                | 31        |
| 4.6 Error Analysis . . . . .                            | 32        |
| <b>5 Conclusions</b>                                    | <b>35</b> |
| <b>References</b>                                       | <b>36</b> |
| <b>Nomenclature</b>                                     | <b>38</b> |
| <b>Appendix</b>                                         | <b>40</b> |

# 1 Introduction and Background

## 1.1 Domestic Ovens

Ovens have become one of the most essential appliances in the kitchen, especially since they cook food without requiring significant attention. A variety of ovens are available on the market, including gas, microwave (which use dielectric heating) and electric devices (which use heating elements).<sup>1</sup> This research project considers domestic electric fan convection ovens (EFCOs), which use heating elements as well as a ventilation fan to circulate hot air around the oven cavity to provide uniform cooking.<sup>2</sup>

The heating elements of an electric oven are usually concealed within the bottom surface (baking element) and exposed on the inside of the top surface (broil element). The purpose of the former is to provide heat to the entire oven cavity to cook food evenly from within, whilst the latter is used to grill / broil food surfaces.<sup>2</sup> Old EFCOs have both baking and broil elements and also have ventilation fans to provide convection

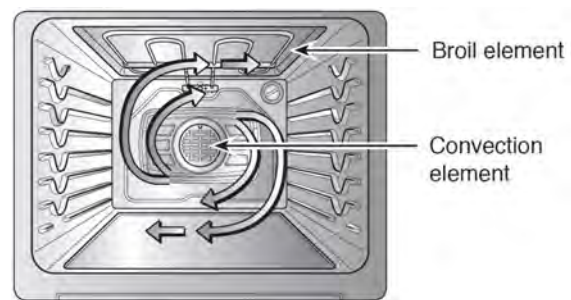


**Figure 1:** *The internal cavity of a ‘true’ electric fan convection oven with a convection element at the back. Image taken from LG.<sup>3</sup>*

throughout the oven. Modern EFCOs are termed ‘true’ EFCOs (TEFCOs), which have a convection (heating) element located around the ventilation fan behind the back panel of the oven<sup>4</sup> [see Figure 1]. Combining convective air flow with heating provides more uniform cooking throughout the oven, as well as reducing the time required to pre-heat. Some newer TEFCOs omit the baking element: this prevents the base of food items such as pastries from charring, as well as reducing the thickness of the oven base, giving a larger oven cavity which is advantageous as oven sizes are constrained to fit in standardised kitchen cavities.<sup>3</sup>

To operate the oven, the cooking temperature is set and the oven pre-heats until that temperature is reached. During cooking, the oven uses mechanical thermostats to regulate the internal temperature [discussed further in Section 2.3] which is measured by a thermocouple on the top surface of the oven cavity.<sup>5</sup> Although there are typically many different cooking modes pre-programmed into a modern oven, this project only considers convection baking, which uses the convection element and the fan to distribute hot air around the food item.<sup>6</sup>

## 1.2 Motivation

### The Need for More Efficient Ovens

Ovens are one of the least energy efficient domestic appliances in the kitchen, with typical efficiencies between 10 – 13%<sup>7</sup> (efficiency is defined as the proportion of energy consumed by the oven which is used to heat up the relevant food item and evaporate water within). Within the EU, oven performance is quantified according to European Standard EN 60350-1:2016/A1:2021. This defines energy ratings (*e.g.* A+, B, C) using an experimental procedure which heats high porosity (HIPOR) bricks initially saturated with moisture from 5 – 55°C.<sup>8</sup> Currently, ovens that attain the highest energy rating only have efficiencies of at most 30%; this is because ratings are defined based on the energy required to heat up the entire oven cavity as opposed to the overall energy consumption of the oven.<sup>8</sup>

Electricity prices in the UK have increased by more than 59% in the last decade;<sup>9</sup> additionally, electricity generation currently accounts for 25% of total worldwide greenhouse gas emissions as 62% of it is generated from burning fossil fuels.<sup>10,11</sup> As such, there is a clear need for more energy efficient ovens to save money and reduce the impact of cooking on the environment.

There have not been many published reports on methods to improve oven efficiency; this is both because oven manufacturers wish to protect their technologies and also because ovens are designed around the EN 60350-1:2016/A1:2021 ratings instead of around the overall energy consumption of the oven. Penssek *et al.* (2005) looked at several different modifications for EFCOs [see Table 1].<sup>12</sup> These individual modifications show comparable energy savings compared to the original base-case; however, even by implementing the best modification (energy consumption reduced by 18.8%), oven efficiencies still do not approach 40%.<sup>12</sup> Since the study only considered individual contributions, there is potential for more energy savings to be realised by combining several of these modifications, although it should be noted that these are unlikely to add linearly.<sup>12,13</sup>

**Table 1:** *Energy saved with oven modifications, after Penssek et al. (2005).<sup>12</sup> Energy consumption was measured over the time required to heat a HIPOR brick from 5 – 55°C.*

| Modification                                        | Energy Consumed (Wh) |
|-----------------------------------------------------|----------------------|
| Standard base-case                                  | 917                  |
| Added 30 mm insulation layer around the oven        | 846 (–7.7%)          |
| Aluminium foil glued over the interior oven surface | 845 (–7.9%)          |
| Triple glazed door                                  | 837 (–8.7%)          |
| Sealing of the door and gaps                        | 801 (–12.6%)         |
| Sealing of the door, gaps and vapour outlet         | 772 (–15.8%)         |
| Control with smaller oscillations                   | 745 (–18.8%)         |

## Cambridge Sensor Innovation

Cambridge Sensor Innovation (CSI) is a company founded by Dr. Mark Williamson to ‘develop sensors and control systems for heat transfer processes’.<sup>14</sup> Their technology is currently used to ‘improve fuel efficiency, reduce greenhouse gas emissions and promote consistent, optimal product quality’.<sup>14</sup> The company has two main goals for domestic ovens: to reduce energy consumption, and to reduce cooking times whilst at the same time improving the quality of the cooked food.<sup>14</sup> It also currently holds patents in areas such as ‘combining infra-red and induction heating systems’, humidity control, residual heat utilisation and heat recovery.<sup>14</sup> Recent work has focused on redesigning the oven altogether, and the PhD project of Dr. Jamie Davidson demonstrated energy savings of up to 30% as well as reductions in cooking times by 75%.

When cooking with ovens, water and volatile lipids within the food items evaporate and are circulated in the air within the cavity. After cooking, this ‘dirty’ air mostly remains inside the oven; however, it also leaks into the kitchen from small vent flows and from opening the oven door. More importantly, as the vent gases cool, these components condense from the vapour and form greasy films on surfaces such as kitchen counter-tops, walls and curtains, which can be difficult to clean. As such, the company has recently created a cooler unit to clean the vent gases leaving the oven cavity [see Figure 2].



**Figure 2:** An oven prototype made by Cambridge Sensor Innovation. Two cooler units (labelled **A** and **B**) slide out of the oven after use. Image taken from Cambridge Sensor Innovation.<sup>14</sup>



## Cambridge Sensor Innovation Cooler Unit

The cooler unit [Figure 3] is a lightweight device made of aluminium, with nylon components including a top cover. During operation, the cooler unit was charged with water at ambient and the top cover isolated the liquid from the surroundings. The inlet of the cooler unit was connected to an outlet made at the back of the oven, and vent gases from the oven passed through the two cooler tubes, transferring thermal energy into the water. Preliminary tests by CSI indicated that the cooler unit water heated up to  $\sim 30^{\circ}\text{C}$  over a typical cooking period of 2 hours, showing that the cooler unit had potential to recover energy; however, this required the utilisation of the heated water (*e.g.* for household chores such as washing dishes or laundry).

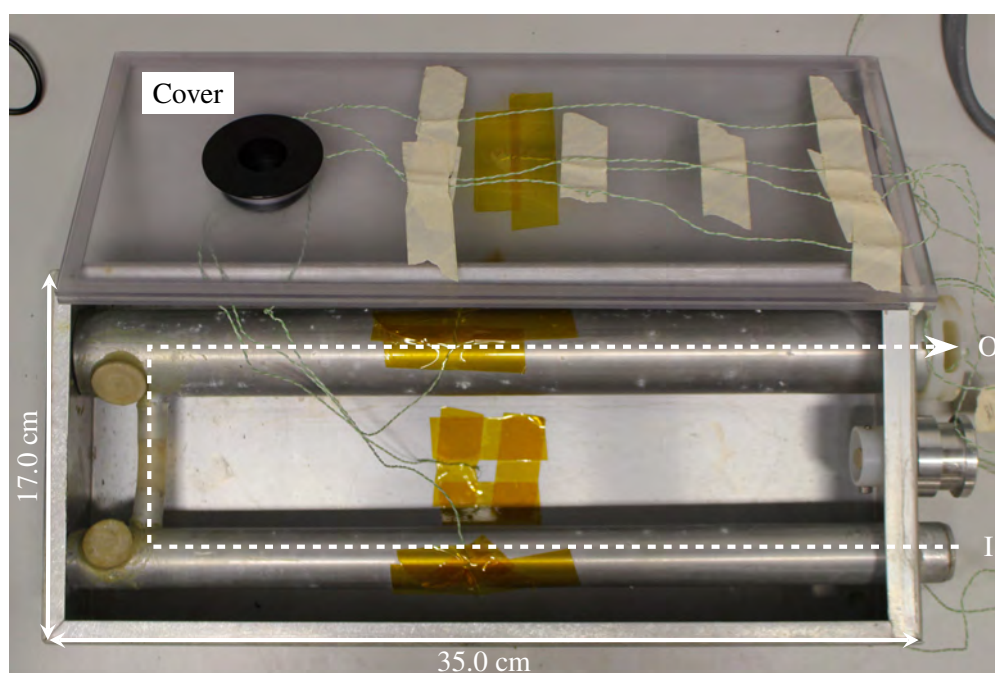


**Figure 3:** *Internal layout of the cooler unit. During operation, the inlet (labelled **I**) is connected to the oven outlet. The cooler unit is filled with water and is sealed with the nylon cover. Vent gases pass through the cooler tubes (path shown with dashed arrow) and leave through the outlet (labelled **O**).*

## 1.3 Project Aims

The first aim of the project was to construct and commission the oven and cooler unit apparatuses. This involved physically connecting the two components as well as wiring up a data logger to measure parameters such as electrical energy consumption and temperature. The system was also fully characterised using energy balances; this ensured that all sources of heat transfer were accounted for and further verified the apparatuses and experimental practices.

The second aim of the project was to verify the theoretical ability of the cooler unit to condense volatile oils and fats. This was done by measuring the temperature of the air leaving the cooler



unit and comparing it with the dew points of lipid-water vapour mixtures emitted by common food items when cooked in ovens. If this temperature was below these dew points and if heat transfer was not rate limited, volatile lipids would theoretically have been condensed within the cooler unit. The last aim of the project was to determine the proportion of ‘useful’ energy from the overall energy consumed by the oven during ‘normal’ operation (cooking). This included the energy that was used to cook the food item and also that recovered within the cooler unit.

## 2 Experimental Methods

Calculations of the rate / amount of heat loss were used in energy balances to characterise the system. Since there were many undefined parameters, experiments were performed in phases [see Table 2] to identify each one in turn.

**Table 2:** *Experimental phases*

| Phase | Description                  | Parameter Solved For                                                                                                                                                                                                                                                                                                                                      |
|-------|------------------------------|-----------------------------------------------------------------------------------------------------------------------------------------------------------------------------------------------------------------------------------------------------------------------------------------------------------------------------------------------------------|
| 1     | Dry runs without cooler unit | $\left\{ \begin{array}{l} \text{Overall heat transfer coefficient of oven back wall } (U_5) \\ \text{Mass flowrate of air exiting the oven top vent } (\dot{M}_2^*) \\ \text{Mass flowrate of air exiting the cooler unit } (\dot{M}_5) \\ \text{Food item design (pseudo-chicken)} \\ \text{Efficiencies } (\eta_c, \eta_r, \eta_T) \end{array} \right.$ |
| 2     | Dry runs with cooler unit    |                                                                                                                                                                                                                                                                                                                                                           |
| 3     | Wet runs without cooler unit |                                                                                                                                                                                                                                                                                                                                                           |
| 4     | Wet runs with cooler unit    |                                                                                                                                                                                                                                                                                                                                                           |

There were two main differences between the experimental phases: ‘dry’ runs were experiments that did not use a food item and runs with the cooler unit were experiments where the cooler unit (charged with water) was connected to the oven.

Each phase involved experiments performed in triplicate, at three set point temperatures (SPTs) commonly used in cooking and baking; 160°C, 200°C, 240°C, giving a total of nine experiments for each phase to establish the effect of temperature on thermal performance.

### 2.1 Apparatuses

#### 2.1.1 Oven Unit

A NEFF oven (model: B12S32N3GB) [Figure 4a] was used as the main cooking appliance. In these experiments, the air vent at the top of the oven cavity was sealed off using Kapton tape (which is thermostable up to 400°C<sup>15</sup>) to ensure that the main sources of heat loss from the oven were conduction through the oven walls and door. A 20.0 mm (OD) hole was drilled into the wall at the back of the oven chamber, and a copper pipe was used to connect it to the internal cavity, providing a male connector to attach to the tubing linked to the cooler unit [see Figure 4b]. To

mimic domestic operation, the oven was placed in a shelving unit and the back of the oven was blanked off by a wooden panel that could be readily removed for access. Holes were also drilled into this panel for the mains power feed and the tubing connecting the oven to the cooler unit.

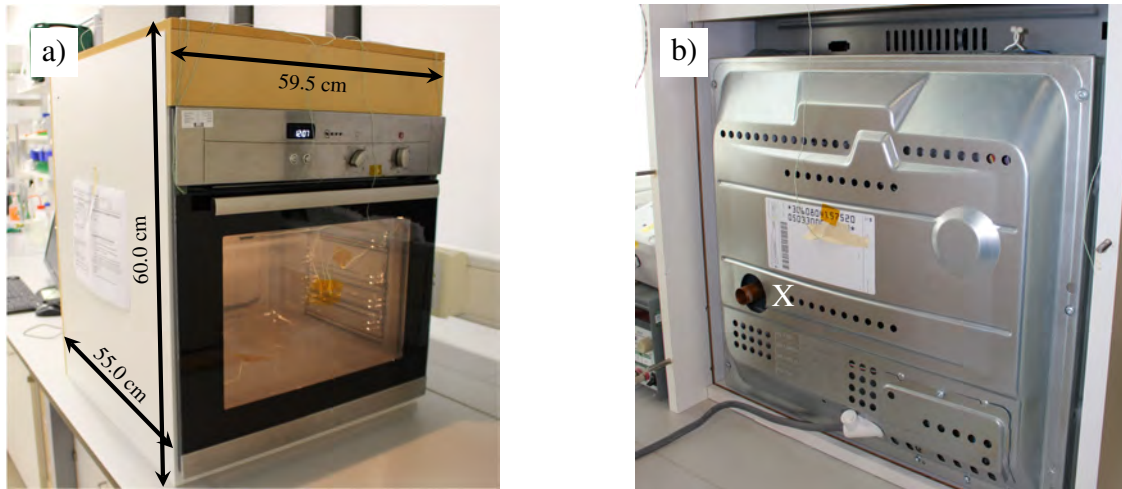


**Figure 4:** The (a) front and (b) back of the oven in its shelving unit. The copper pipe at the back of the oven chamber is labelled X.

The original oven door was constructed of three glass panels separated by two narrow air gaps. Unfortunately, when installing thermocouples for temperature measurements, the inner glass panel shattered and was removed. Since the oven model used was not new (first sold in 2015<sup>16</sup>) and the middle and outer glass panels were still intact, it was decided that sourcing a replacement door was not an option as it would delay the experiments. Additionally, it was decided that this incident would not affect the main aim of the research project, which was ‘to develop research skills and experience the trials, tribulations and satisfactions of original research’.<sup>17</sup>

### 2.1.2 Cambridge Sensor Innovation Cooler Unit

Modifications were made to the original CSI cooler unit to allow for more accurate and easier measurements to be made. The original design used a stainless-steel handle attached to the main body of the cooler unit by nylon pieces so that the cooler unit could slide out of the oven with ease. The handle, the connecting pieces and the welded screws holding them



**Figure 5:** The cooler unit with insulation

together were removed. The aluminium body was insulated with nitrile foam rubber, with thicknesses of 2.5 cm on the sides, 1.0 cm on the top, bottom and front surfaces, and 15.0 cm for the back surface (this was due to the shape the rubber sheets were delivered in). The insulation was

secured in place using a cardboard wrap [see Figure 5], which also provided easy access to the cooler unit.

The cooler unit was placed behind the oven on top of a tray to collect any water leaks; this tray also served to locate the unit level with the outlet port of the oven to minimise kinetic energy losses of the air. This was because the air mass flowrate was relatively slow, and even small pressure differences could stop air flow altogether; detailed design of the fan and air ducting would be needed for an oven fitted with cooler units.

### 2.1.3 Oven-Cooler Unit Connection

The cooler unit was connected to the oven by a 25.0 mm (OD) silicone tube [labelled 7 in Figure 6]. The tubing was 20.0 cm long and was insulated by 2.0 mm thick nitrile foam rubber held in place by cable ties. A K type thermocouple measured the temperature at the outer wall of tubing, inside the insulation layer and a 'T'-junction piece allowed the temperatures of the air at the centre of the tubing and at the inlet of the cooler unit to be measured.

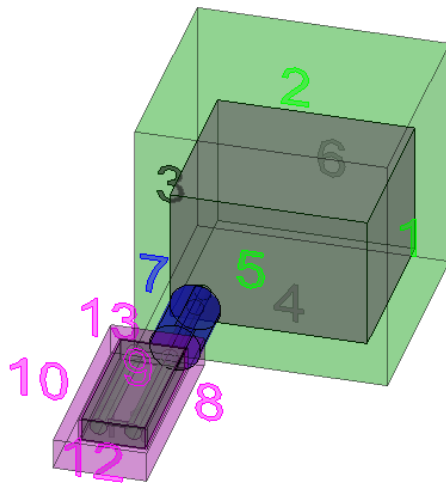


**Figure 6:** 3D schematic of the oven with the cooler unit. Key in Table 3.

| Number | Surface              |
|--------|----------------------|
| 1      | Oven (left)          |
| 2      | Oven (top)           |
| 3      | Oven (right)         |
| 4      | Oven (bottom)        |
| 5      | Oven (back)          |
| 6      | Oven (door)          |
| 7      | Tubing               |
| 8      | Cooler Unit (left)   |
| 9      | Cooler Unit (top)    |
| 10     | Cooler Unit (right)  |
| 11     | Cooler Unit (bottom) |
| 12     | Cooler Unit (back)   |
| 13     | Cooler Unit (front)  |

**Table 3:** List of heat transfer surfaces

## 2.2 Measurements

### 2.2.1 Temperature and Power

Surface temperatures were monitored using K type thermocouples in order to calculate the rates and amount of heat lost across each surface. Values of the electrical energy consumption were also required to calculate the rates and amount of energy supplied to the oven. Both of these were measured simultaneously using a data logger [Figure 7] previously constructed by Dr. Jamie Davidson, which was controlled by an Arudino micro microcontroller.

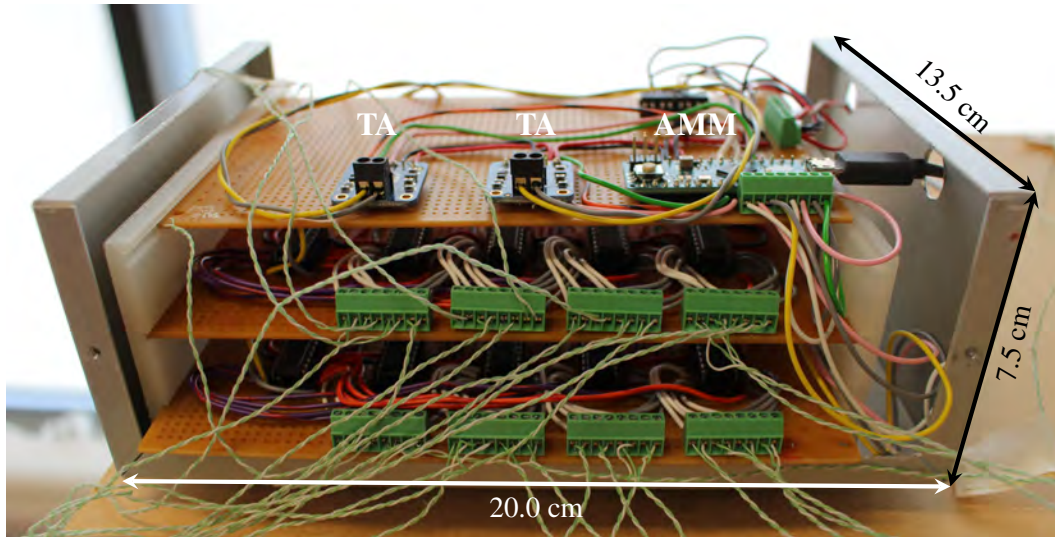


**Figure 7:** Data logger with top cover removed. The top shelf includes two thermocouple amplifiers (labelled **TA**) and the Arduino microcontroller (labelled **AMM**). The bottom two shelves hold the thermocouple connectors.

The thermocouple junctions were fabricated from perfluoroalkoxy insulated thermocouple wire. These were cut into separate pieces and the tips were connected using an arc welder. Thirty-two thermocouple pieces were connected and screwed into individual slots on the bottom two shelves of the data logger. Most of the thermocouples were fixed to walls (*e.g.* internal and external walls of the oven; internal and external walls of the cooler unit and its insulation) using Kapton tape, whilst others were left suspended to measure the temperature of the air (*e.g.* in the middle of the tubing connection; at the exit of the cooler unit) or water (*e.g.* three at locations inside the cooler unit; in the food item).

The data logger was connected to a desktop PC running a Python program written by Dr. Jamie Davidson to record and process the data [see Appendix]. The program provided live plotting of the energy used through cumulative energy plots (CEPs) and of the temperatures through thermal history plots (THPs). When recording data, the thermocouple voltages were sampled every few hundred milliseconds in their processing order (*i.e.* left to right slot, bottom to top shelf). Two thermocouple amplifiers read the voltage and this signal was then converted into serial data read by the microcontroller as temperatures. The electrical power was measured by a Grasslin taxxo ER 80-1 power meter which was connected to the data logger separately via an isolated connection to protect the microcontroller from the mains voltage.

### 2.2.2 Air Flowrate

A bubble flowmeter was used to measure the flowrate of the air exiting the cooler unit. Traditional air flow measurement devices could not be used due to the small air flowrate and the small pressure

drops involved. Bubble flowmeters are fairly simple to construct as they rely on simple principles to measure flowrate. The device consists of a long vertical cylindrical tube with an open end at the top, as well as an inlet at the bottom entering the tube from the side. A small reservoir of surfactant solution sits just below the inlet, and its level can be controlled using a pipette bulb. As air is fed in, it passes without resistance up the cylinder and exits from the top. When the pipette bulb is squeezed, the surfactant solution rises and temporarily covers the inlet. The air flow forces a film of solution to form, spanning the cylinder. Since the thickness of the film is on the order of  $O(100\text{ nm})$ ,<sup>18</sup> the weight of the film is negligible, and so it imposes negligible resistance to the flow of air. As the film travels up the cylinder with the air, its speed can be calculated by measuring the time taken for the film to travel a pre-marked distance, which then gives the volumetric flowrate [see Section 3.2 for calculations]. The bubble flowmeter used was connected to the outlet of the cooler unit via a reducing coupling (35.0 mm to 7.0 mm OD); a thermocouple was also used at this point to evaluate the density of the air entering the bubble flowmeter.

## 2.3 Main Experimental Campaigns

At the beginning of each run, the oven-cooler unit connection and oven top vent were sealed off using bungs and Kapton tape. At the end of each run, the oven SPT was set to ambient and the oven was left open. The bungs, Kapton tape, cooler unit (if connected) and the food item (if used) were removed; the ventilation fan was also allowed to run and cool the oven down before the next run. Several runs were also done under ‘normal’ operation with the oven top vent open; any parameters derived from these experiments have been notated with a \*.

### Phase 1

Phase 1 experiments involved dry runs without the cooler unit, and their purpose was to quantify the thermal performance of the oven by itself. The overall heat transfer coefficient for the back wall for the oven was calculated as it could not be easily estimated due to the number of components and air gaps it contained. This was done by forming an inverse problem using all the energy balances across the nine runs in order to find an average value. To perform these energy balances, the oven was allowed to reach steady state, which was achieved when both the internal and external oven wall temperatures remained constant over time (the period of time leading up to steady state is referred to as the transient state). Constant values were not seen for the internal oven wall temperatures as ovens operate under ON-OFF control (OOC) since these control systems are cheap, reliable and in widespread use.<sup>19</sup> The principles of OOC were the same through both the transient and steady states: the convection element only turned on when the internal temperature reached

a pre-defined offset below the SPT. Following this, once the internal temperature exceeded a pre-defined offset above the SPT, the convection element turned off and the oven cavity cooled down<sup>i</sup>. Hence, steady state temperatures for the oven internal walls were defined by taking averages of the temperatures.

For each run, the oven was run for 4500 s, allowing for 3500 s in the transient state and 1000 s in steady state so that accurate averages of the temperatures could be measured (the lengths of the steady state periods varied on the order of  $O(10\text{ s})$  between the runs to allow for an integer number of OOC cycles to be included in the average). Similar runs were also performed with the oven top vent open to estimate the vent flowrate exiting the oven during ‘normal’ operation.

## Phase 2

Phase 2 experiments involved dry runs with the cooler unit, and their purpose was to quantify the mass flowrate of air exiting the cooler unit. As the apparatus now contained water inside the cooler unit, batch calculations were required as the heat capacity of water is large and would take up to 5 hours to achieve steady state (which would be both impractical and unrealistic for domestic use).

At the beginning of each run, the cooler unit was filled with 2000 g of water and was insulated. To mimic the actual operation of the cooler unit (which is only used during cooking and not when the oven is preheating), the oven was turned on for 12000 s, allowing for 4500 s in the pre-heating stage, before swiftly connecting the cooler unit to the oven after removing the bung and Kapton tape at the oven exit. This quick transition minimised the amount of heat lost to the surroundings from hot air exiting the oven, and the cooler unit was heated for 7500 s (125 min, a typical cooking time) in the ‘cooking’ stage. After the cooler unit was installed, the bubble flowmeter was attached at regular intervals and air measurements were made; this was repeated nine times over the ‘cooking’ stage.

## Phase 3

Phase 3 experiments involved wet runs without the cooler unit and were performed to design the food item. HIPOR bricks utilised in the EN 60350-1:2016/A1:2021 standard were beyond the project budget, leading to the use of a pseudo food item based on raw chicken, hence referred to as the pseudo-chicken. Separate tests conducted at home indicated that a whole raw chicken, weighing  $\sim 1400\text{ g}$ , when cooked in a TEFCO at a SPT of  $180^\circ\text{C}$ , lost 200 g of mass (assumed

---

<sup>i</sup>During the transient state, the ‘equilibrium’ temperature of the OOC began higher than the SPT before decreasing towards it as steady state was approached.

to mainly be water) after 80 min (4800 s); hence the pseudo-chicken was developed to mimic this performance. A Pyrex® tray weighing 1429 g was used as the ‘dry’ pseudo-chicken and it was filled with 200 g of water for each run. This setup was used as a benchmark, and later design iterations used kitchen foil to reduce the rate of water evaporation. The main difference between these iterations was the number and size of the perforations on the top kitchen foil layer of the pseudo-chicken, which tuned the evaporation rate. A regular array of hole positions was marked on the foil sheet and was created using a metal rod, with callipers confirming the diameters.

Before each run, the pseudo-chicken was placed inside the oven on top of the centre tray. The oven was turned on with a SPT of 180°C, and after 4800 s, the pseudo-chicken was reweighed to measure the mass of water lost. After identifying the design that *just* evaporated all 200 g of water within 4800 s, it was further evaluated and verified using an evaporation rate plot (ERP). The amount of water evaporated after different ‘cooking’ periods was measured and trends in the evaporation rate helped fine tune and confirm the final design. The experimental method for this was identical to the original Phase 3 experiments, however the pseudo-chickens were reweighed after being ‘cooked’ for 1200 s, 2400 s and 3600 s instead.

To determine the performance of the experiments, energy balances were also done at the SPTs, allowing the oven 4500 s in the pre-heating stage before swiftly placing the pseudo-chicken inside it to ‘cook’ for a further 7500 s in the ‘cooking’ stage. Separate runs were also performed with the oven top vent open to provide a representative comparison for ‘normal’ operation.

## **Phase 4**

Phase 4 experiments involved wet runs with the cooler unit, and their purpose was to determine the efficiencies of the oven, the cooler unit and the overall system. At the beginning of each run, the pseudo-chicken was loaded with 500 g of water and the cooler unit was charged with 2000 g of water. The oven was turned on for 12000 s, allowing for 4500 s in the pre-heating state, before swiftly placing the pseudo-chicken inside the oven and connecting the cooler unit; heating continued for a further 7500 s in the ‘cooking’ stage.



### 3 Calculations

#### 3.1 Heat Transfer Coefficients

To calculate rates of heat loss ( $Q_i$ ) through the thirteen different surfaces [refer to Table 3], overall heat transfer coefficients ( $U_i$ ) were estimated. The surfaces in the system were considered to follow Newton's law of cooling [Equation 1]. It was also assumed that the surfaces were at uniform temperatures, the temperature gradients ( $\Delta T_i$ ) across the surfaces were linear, and  $U_i$ s did not change over time.

$$Q_i = A_i U_i \Delta T_i \quad (1)$$

where  $A_i$  represents the area for heat transfer for surface  $i$ .

##### Oven Sides (Surfaces 1 – 4)

Surfaces 1 – 4 were constructed from three layers: an inner steel wall, a layer of insulation and an outer steel wall [Figure 8]. Their thicknesses ( $d_i$ ) were measured through partially disassembling the oven and  $U_i$  was calculated as thermal conductivities ( $k_i$ ) in series.

$$\frac{1}{U_i} = \frac{d_{i,in}}{k_{steel}} + \frac{d_{i,mid}}{k_{wool}} + \frac{d_{i,out}}{k_{steel}} \quad i \in \{1 - 4\} \quad (2)$$

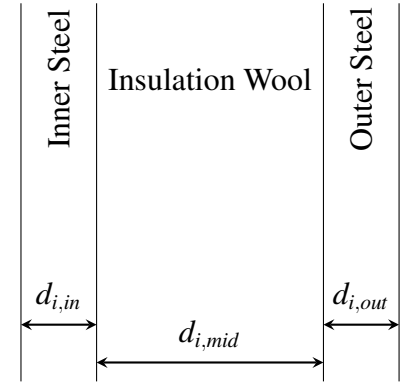


**Figure 8:** Model of the oven sides

##### Back Wall of the Oven (Surface 5)

It was impractical to use the previous model for the back wall of the oven as it featured many air gaps to accommodate components such as the ventilation fan, the convection element and wiring. Hence, the overall heat transfer coefficient of this surface ( $U_5$ ) was calculated by an inverse problem. This used an energy balance between the power supplied to the oven ( $P_{av}$ ) and the rate of heat loss of the oven by conduction through the oven walls and door ( $Q_{lost,oven}$ ); the  $U_5$  value was then estimated by difference.

$$P_{av} = Q_{lost,oven} \quad (3)$$

$$U_5 = \frac{P_{av} - \sum_{i=1}^6 A_i U_i (T_{i,in} - T_{i,ex})}{A_5 (T_{5,in} - T_{5,ex})} \quad (4)$$

where  $T_{i,in}$ ,  $T_{i,ex}$  represent the internal and external surface temperatures of wall  $i$ .  $U_5$  values from all the runs done at the SPTs were averaged out to give an overall  $U_5$ .

## Oven Door (Surface 6)

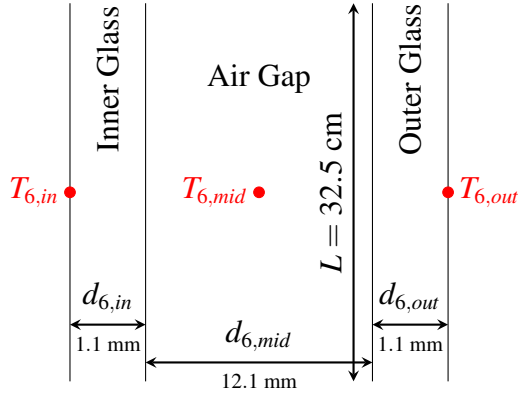


**Figure 9:** Model of the oven door

The model of the oven door [Figure 9] was similar to that of surfaces 1 – 4, with glass panes replacing the steel walls. However, the same model could not be applied as the air gap between the two panes transfers heat by natural convection as well as conduction. The door could also be modelled as resistances in parallel, but the heat transfer coefficient of the air gap (provided by the Nusselt number) needed to be determined first.

Winterton (1997) provides the result for the Nusselt number of a narrow enclosed air gap ( $Nu_{6,mid}$ ):<sup>20</sup>

$$Nu_{6,mid} = [1 + (0.0605 Ra_6^{0.33})^m]^{\frac{1}{m}} \quad (5)$$

$$Ra_6 = Gr_6 \times Pr_6 = \frac{d_{6,mid}^3 g \beta (T_{6,in} - T_{6,ex}) Pr_6}{\nu^2} \quad (6)$$

$$m = \left[ \frac{L}{d_{6,mid}} \right]^{0.45} \quad (7)$$

$$\frac{1}{U_6} = \frac{d_{6,in}}{k_{glass}} + \frac{d_{6,mid}}{Nu_{6,mid} k_{air}} + \frac{d_{6,out}}{k_{glass}} \quad (8)$$

where  $Ra_6, Gr_6, Pr_6$  are the Rayleigh, Grashof and Prandtl numbers across the door air gap;  $m$  a correlation coefficient;  $g$  the acceleration due to gravity;  $\beta$  the thermal expansion coefficient of the air in the gap and  $\nu$  the kinematic viscosity of the air in the gap.

## Other (Surfaces 7 – 13)

As the remaining walls were made from only one material (with thickness  $d_i$ ), their heat transfer coefficients ( $h_i$ ) were calculated using thermal conductivities found from product specifications [see Table 4]; a simple definition for  $h_i$  was used [see Equation 9].

**Table 4:** Thermal conductivities of materials<sup>21,22</sup>

| Material           | Thermal Conductivity ( $\text{W m}^{-1} \text{K}^{-1}$ ) |
|--------------------|----------------------------------------------------------|
| Stainless-Steel    | 13.4                                                     |
| Insulation Wool    | 0.12                                                     |
| Glass              | 1.4                                                      |
| Nitrile Insulation | 0.04                                                     |

$$h_i = \frac{k_i}{d_i} \quad i \in \{7 - 13\} \quad (9)$$

## 3.2 Air Flowrates

### Leaving the Top Vent of the Oven (During ‘Normal’ Operation)

The difference between the power supplied to the oven with ( $P_{av}$ ) and without sealing the top vent ( $P_{av}^*$ ) gave the rate of energy which was transported out of the oven through the top vent during ‘normal’ operation. A simple sensible heat change calculation was used to calculate the mass flowrate of the air leaving the top vent of the oven ( $\dot{M}_2^*$ ).

$$\dot{M}_2^* = \frac{P_{av}^* - P_{av}}{Cp_{air,centre}(T_{centre} - T_{ambient})} \quad (10)$$

where  $Cp_{air,centre}$  is the thermal heat capacity of air at the centre of the oven;  $T_{centre}$  the temperature of air at the centre of the oven and  $T_{ambient}$  the temperature of air at ambient.

### Leaving the Cooler Unit

A model of the observed section of the bubble flowmeter [Figure 10] was used to calculate the mass flowrates. The speed at which the film rose was calculated by measuring the time ( $\Delta t$ ) it took to travel between two marked lines on the cylinder. It was assumed that this speed was equal to the speed at which the air was travelling at (due to negligible flow resistance), and hence the mass flowrate ( $\dot{M}_5$ ) was calculated from the cross-sectional area of the cylinder.

$$\dot{M}_5 = \rho_{air} \frac{\pi D^2}{4} \frac{H}{\Delta t} \quad (11)$$

where  $\rho_{air}$  is the density of the air;  $D$  the flowmeter diameter and  $H$  the distance between the two marked lines on the cylinder.

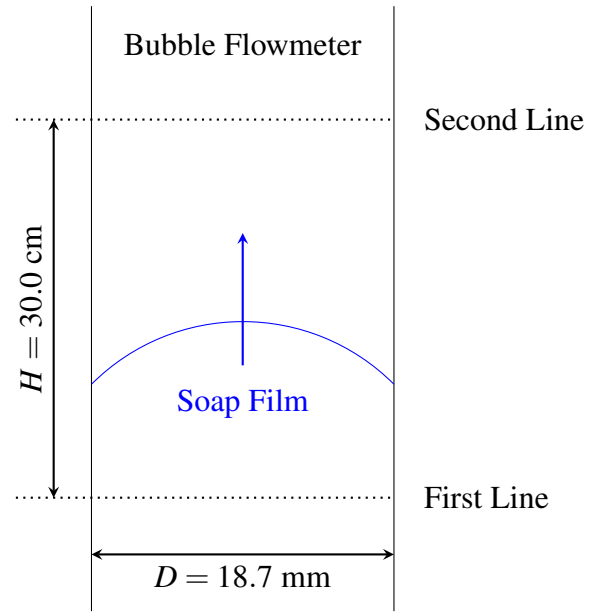


**Figure 10:** A model of the measurements section of the bubble flowmeter

## 3.3 Energy Balances

Energy balances were done to analyse the individual contributions of the different sources of heat transfer and to determine whether all energy losses were accounted for. Discrepancies were used to quantify the differences between the measured energy consumption of the oven with the calculated

energy usage and loss. They were also used to identify potential sources of random and systematic errors. Discrepancies were defined either based on power ( $\delta_{P,1}$  in Phase 1) or by energy ( $\delta_{E,j}$  in Phases 2 – 4), and when quoted as percentages ( $\delta_{P,1,\%}$ ,  $\delta_{E,j,\%}$ ) represent the proportion of the discrepancy as a fraction of the input average power ( $P_{av,1}$ ) or energy ( $E_{T,j}$ ).

$$\delta_{P,1,\%} = \frac{\delta_{P,1}}{P_{av,1}} \quad \text{or} \quad \delta_{E,j,\%} = \frac{\delta_{E,j}}{E_{T,j}} \quad j \in \{2 - 4\} \quad (12)$$

### Heat Fluxes from the Surfaces

In general, the surfaces lost heat by natural convection and radiation. In these experiments, radiation was ignored as the radiative heat fluxes emitted from the surfaces were negligible compared to the convective heat fluxes from the surfaces.

If radiative heat fluxes were accounted for, complex calculations involving different surfaces found in the laboratory would need to be taken into account; however, since most of the surfaces of the apparatuses were close to room temperature, the radiative fluxes emitted and received by these surfaces remained constant over time. Additionally, the surface materials had low emissivities (*e.g.*  $0.1 < \varepsilon < 0.2$  for aluminium<sup>23</sup>), suggesting that the mechanism for heat loss in the experiment could be modelled using conduction alone.

The result for the Nusselt number of natural convection on a vertical surface ( $Nu_{i,conv}$ ) is given by Churchill and Churchill (1975).<sup>24</sup> This allowed the overall rate of convective heat loss from the external oven wall surfaces to be calculated, providing an additional check for the overall rates of heat loss as well as verifying that radiative heat fluxes could be ignored.

$$Nu_{i,conv}^{\frac{1}{2}} = \sqrt{0.68} + \frac{\left(\frac{Ra_{i,conv}}{5}\right)^{\frac{1}{6}}}{\left[1 + \left(\frac{0.5}{Pr_{i,conv}}\right)^{\frac{9}{16}}\right]^{\frac{8}{27}}} \quad (13)$$

where  $Ra_{i,conv}$ ,  $Pr_{i,conv}$  are the Rayleigh and Prandtl numbers over the vertical surface.

### Phase 1

The energy balance for Phase 1 runs represented the simplest case and used steady state calculations with the average power. The only expected source of heat loss was conduction through the oven walls and door ( $Q_{lost,oven}$ ), and since the oven operated under OOC, averages were taken for the internal wall temperatures ( $T_{i,in}$ ) over the periods of steady state.

$$Q_{lost,oven} = \sum_{i=1}^6 A_i U_i (T_{i,in} - T_{i,ex}) \quad (14)$$

$$\delta_{P,1} = P_{av,1} - Q_{lost,oven} \quad (15)$$

## Phase 2

With the cooler unit attached, the energy balance for Phase 2 became more complex and involved batch calculations instead of steady state calculations as the temperature of the water in the cooler unit varied over time. Additionally, this meant that the temperature variation from the OOC could no longer be simply calculated using an average, but instead by using an integral over time.

The expected sources of heat loss included those in Phase 1 (but in the form of energy instead of a rate of energy loss,  $E_{lost,oven}$ ), as well as heat loss by conduction through the oven-cooler unit connection ( $E_{lost,tubing}$ ), conduction through the cooler unit walls ( $E_{lost,cu}$ ), and the air leaving the cooler unit ( $E_{lost,air}$ ).

$$E_{lost} = E_{lost,oven} + E_{lost,tubing} + E_{lost,cu} + E_{lost,air} \quad (16)$$

where:

$$E_{lost,oven} = \sum_{i=1}^6 A_i U_i \int_{t_s}^{t_f} (T_{i,in} - T_{i,ex}) dt \quad (17)$$

$$E_{lost,tubing} = \pi D_{tubing} h_{tubing} \int_{t_s}^{t_f} \int_{x=0}^{x=X} (T_{7,x,in} - T_{7,x,ex}) dx dt \quad (18)$$

$$E_{lost,cu} = \sum_{i=8}^{13} A_i h_i \int_{t_s}^{t_f} (T_{i,in} - T_{i,ex}) dt \quad (19)$$

$$E_{lost,air} = \dot{M}_5 \int_{t_s}^{t_f} \int_{T_{cu,outlet,s}}^{T_{cu,outlet,f}} C_{p,air,cu,outlet} dT dt \quad (20)$$

with  $t_s, t_f$  representing the start and finish times for batch calculations;  $D_{tubing}$  the diameter of the oven-cooler unit tubing connection;  $x$  a position coordinate along the length of the tubing;  $X$  the total length of the tubing;  $T_{7,x,in}, T_{7,x,ex}$  the internal and external surface temperatures of the insulation on the tubing at a position  $x$ ;  $T_{cu,outlet,s}, T_{cu,outlet,f}$  the initial and final temperatures of the air leaving the cooler unit and  $C_{p,air,cu,outlet}$  the thermal heat capacity of the air leaving the cooler unit.

The sensible heating of the cooler unit water represented heat energy that was recovered from the experimental runs ( $E_{recovered}$ ):

$$E_{recovered} = M_{cu,w} \int_{T_{cu,w,s}}^{T_{cu,w,f}} C_{p,w} dT_{cu,w} \quad (21)$$

where  $M_{cu,w}$  is the mass of the water inside the cooler unit;  $T_{cu,w,s}$ ,  $T_{cu,w,f}$  the initial and final temperatures of the water inside the cooler unit and  $Cp_w$  the thermal heat capacity of water.

Hence:

$$\delta_{E,2} = E_{T,2} - E_{lost} - E_{recovered} \quad (22)$$

### Phase 3

The energy balance of Phase 3 also involved batch calculations instead of steady state calculations as the amount of water in the pseudo-chicken changed over time [see Equation 23]. The only source of heat loss was conduction through the oven walls and door whereas the only source of heat use was to ‘cook’ the pseudo-chicken ( $E_{cooking}$ ), this consisted of three contributions:

- (a) the sensible heating of the Pyrex<sup>®</sup> tray
- (b) the sensible heating of the pseudo-chicken water up to its boiling point ( $T_{boil} = 100^\circ\text{C}$ )
- (c) the latent heating required to evaporate the pseudo-chicken water

$$E_{cooking} = \overbrace{M_{pc,py} \int_{T_{pc,py,s}}^{T_{pc,py,f}} Cp_{py} dT}^{(a)} + \overbrace{M_{pc,w,s} \int_{T_{pc,w,s}}^{100} Cp_w dT_{pc,w}}^{(b)} + \overbrace{(M_{pc,w,s} - M_{pc,w,f})\lambda_w}^{(c)} \quad (23)$$

where  $M_{pc,py}$  is the mass of the Pyrex<sup>®</sup> tray;  $T_{pc,py,s}$ ,  $T_{pc,py,f}$  the initial and final temperatures of the Pyrex<sup>®</sup> tray;  $Cp_{py}$  the thermal heat capacity of the Pyrex<sup>®</sup> tray;  $M_{pc,w,s}$ ,  $M_{pc,w,f}$  the initial and final masses of water inside the pseudo-chicken;  $T_{pc,w,s}$  the initial temperature of the water inside the pseudo-chicken and  $\lambda_w$  the latent heat of evaporation of water.

Hence:

$$\delta_{E,3} = E_{T,3} - E_{lost,oven} - E_{cooking} \quad (24)$$

### Phase 4

The final energy balance brought components from all the previous energy balances together. These contributions included:

- all four sources of heat loss as in Phase 2 [see Equation 16]
- heat recovered in the cooler unit water [see Equation 21]
- heat used to ‘cook’ the pseudo-chicken [see Equation 23]

Hence:

$$\delta_{E,4} = E_{T,4} - E_{lost} - E_{recovered} - E_{cooking} \quad (25)$$

### 3.4 Efficiencies

Efficiencies were defined to characterise the performance of the system:

- (i) Oven cooking efficiency ( $\eta_c$ ) - terms in [square brackets] were omitted for Phase 3 experiments

$$\eta_c = \frac{E_{cooking}}{E_{lost} + [E_{recovered}] + E_{cooking}} \quad (26)$$

- (ii) Cooler unit / recovered efficiency ( $\eta_r$ ) - terms in {braces} were omitted for Phase 2 experiments

$$\eta_r = \frac{E_{recovered}}{E_{lost} + E_{recovered} + \{E_{cooking}\}} \quad (27)$$

- (iii) Total oven efficiency ( $\eta_T$ ) - terms in [square brackets] were omitted for Phase 3 experiments

$$\eta_T = \eta_c + [\eta_r] = \frac{E_{cooking} + [E_{recovered}]}{E_{lost} + [E_{recovered}] + E_{cooking}} \quad (28)$$

### 3.5 Cooler Unit Heat Exchanger Models

The performance of the cooler unit was likened to that of a heat exchanger. Two simple models were used to quantify the overall conductance ( $UAF$ ) of the cooler unit calculated from the duty ( $(UAF)_{cu,duty}$ ) and from the rate of heat transfer to the cooler unit water ( $(UAF)_{cu,w}$ ).

#### From the Duty

$$(UAF)_{cu,duty} = \frac{\dot{M}_5 [Cp_{air,in}(T_{cu,inlet} - T_{ambient}) - Cp_{air,out}(T_{cu,outlet} - T_{ambient})]}{\Delta T_{cu,lm}} \quad (29)$$

where:

$$\Delta T_{cu,lm} = \frac{(T_{cu,inlet} - T_{cu,w}) - (T_{cu,outlet} - T_{cu,w})}{\ln \left( \frac{T_{cu,inlet} - T_{cu,w}}{T_{cu,outlet} - T_{cu,w}} \right)} \quad (30)$$

with  $F$  representing a correction factor;  $\Delta T_{cu,lm}$  the log mean temperature difference of the cooler unit;  $Cp_{air,in}, Cp_{air,out}$  the thermal heat capacity of air at the inlet and outlet of the cooler unit and  $T_{cu,inlet}, T_{cu,outlet}$  the temperatures of air at the inlet and outlet of the cooler unit.

#### From the Rate of Heat Transfer to Cooler Unit Water

$$(UAF)_{cu,w} = \frac{\frac{d}{dt}(M_{cu,w} Cp_w T_{cu,w})}{\Delta T_{cu,lm}} \quad (31)$$

Since these models described  $UAF$  values at each point in time, they were averaged out to give overall values of  $UAF$ .



## 4 Results and Discussion

### 4.1 Phase 1

#### System Behaviour

It was assumed that the main consumer of energy was the convection element, with negligible energy consumed by the LCD screen and the light bulb in the roof of the oven cavity. In the first  $\sim 750$  s, the mains supplied energy at constant power to the oven to heat the oven cavity. Once the internal temperature reached the oven set point temperature ( $T_{sp}$ ), the oven employed OOC and the heating element was cyclically turned on and off [see Figures 11a, 11b and 11c].

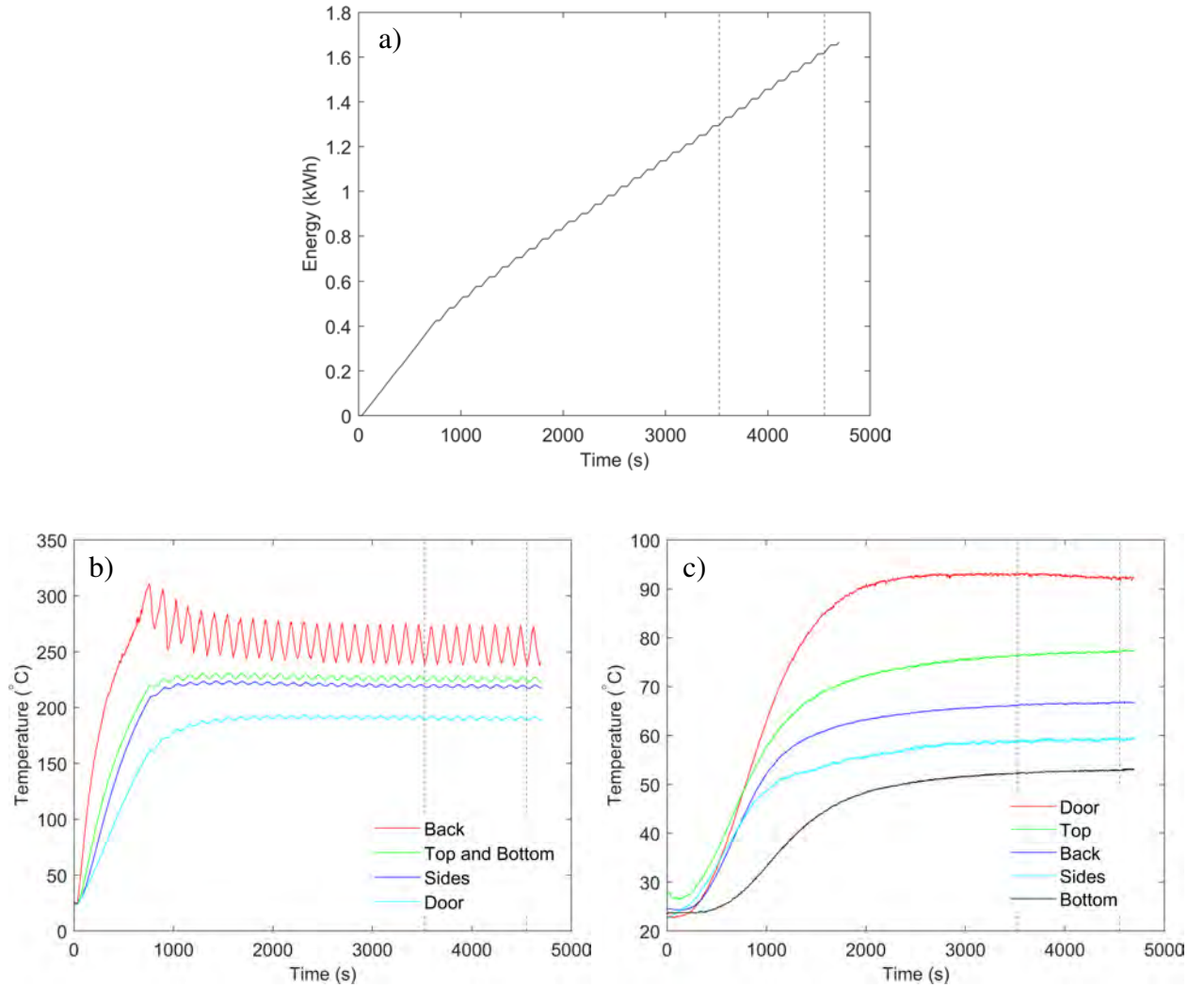


**Figure 11:** Phase 1 run with  $T_{sp} = 240^{\circ}\text{C}$ : (a) cumulative energy plot; (b) internal thermal history plot; (c) external thermal history plot. The period over which steady state calculations were done is indicated by the dashed lines.

Although the internal wall temperatures reached steady state after  $\sim 1750$  s, the steady state calculations were performed between  $\sim 3500$  s and  $\sim 4500$  s. This was because the transients in the external oven wall temperatures lasted twice as long as those in the internal wall temperatures due to the thermal lag provided by the oven walls.

### Oven Overall Heat Transfer Coefficients

Table 5 reports the  $U_i$  values calculated for the different surfaces at  $T_{sp} = 240^\circ\text{C}$ . The back surface and the oven door had noticeably larger values, while the other walls were comparable. The  $U_i$  values were all observed to be independent of  $T_{sp}$  except for that of the oven door which varied by 1.3%, as the Rayleigh number in the Winterton (1997) correlation is temperature dependent [refer to Equation 6].

**Table 5:** Overall heat transfer coefficients of the oven surfaces with  $T_{sp} = 240^\circ\text{C}$ . Numeric labels refer to Table 3.

| Surface ( $i$ ) | $U_i$ ( $\text{W m}^{-2} \text{K}^{-1}$ ) |                              |                              |
|-----------------|-------------------------------------------|------------------------------|------------------------------|
|                 | $T_{sp} = 160^\circ\text{C}$              | $T_{sp} = 200^\circ\text{C}$ | $T_{sp} = 240^\circ\text{C}$ |
| Left (1)        | $5.79 \pm 0.50$                           |                              |                              |
| Top (2)         | $3.87 \pm 0.34$                           |                              |                              |
| Right (3)       | $5.79 \pm 0.50$                           |                              |                              |
| Bottom (4)      | $2.11 \pm 0.18$                           |                              |                              |
| Back (5)        | $10.44 \pm 0.91$                          |                              |                              |
| Door (6)        | $21.81 \pm 0.04$                          | $22.97 \pm 0.03$             | $23.96 \pm 0.05$             |

The oven surfaces have different primary purposes. The oven sides (left, right, top and bottom) insulate the oven; the back surface provides heating (from the convection element) and the oven door allows the user to observe their food whilst cooking. Therefore, the back and the oven door were expected to have higher  $U_i$  values than the sides. In fact, the back was designed to be less resistive to heat transfer so that electrical components such as the fan motor and its circuitry do not overheat.

$U_5$  was verified by comparison with studies in the literature such as Cernela *et al.* (2013)<sup>25</sup> featuring a domestic TECFO who reported a  $U_5$  value of  $11.6 \text{ W m}^{-2} \text{K}^{-1}$ . Although  $U_5$  was expected to be larger than  $U_i$  for surfaces 1 – 4, it was expected to be similar to  $U_6$ : the same study done by Cernela *et al.* (2013)<sup>25</sup> with  $T_{sp} = 240^\circ\text{C}$  reported a  $U_6$  value of  $10.2 \text{ W m}^{-2} \text{K}^{-1}$ .  $U_6$  was thus  $\sim 2\times$  larger than expected and this attributed to the damaged oven door which lacked a third glass pane and an additional air gap.

## Energy Balance

The relative proportions of energy lost via the different surfaces [Figure 12] were consistent across the SPTs. Although  $U_6$  was greater than  $U_5$ , both surfaces lost similar amounts of energy, which can be explained by the temperature difference across these walls ( $\Delta T = T_{i,in} - T_{i,ex}$ ).

Taking the run with a  $T_{sp} = 240^\circ\text{C}$ , the  $\Delta T$  across the oven door was 98.5 K, whereas the  $\Delta T$  across the back surface was 197.2 K. For the internal temperatures

(door:  $188.3^\circ\text{C}$  and back:  $255.5^\circ\text{C}$ ), the back surface was hotter due to the presence of the convection element, whereas for the external temperatures (door:  $89.8^\circ\text{C}$  and back:  $58.3^\circ\text{C}$ ), the faulty door was hotter due to the missing glass pane and air gap. The error of the doubled  $U_i$  was negated by the effect of the halved  $\Delta T_i$ , bringing the rates of heat loss of these two surfaces closer together, hence explaining why both surfaces lost similar amounts of heat.

The average energy consumption of the oven from runs with a  $T_{sp} = 240^\circ\text{C}$  was measured at 1.12 kW and the estimated rate of heat loss from the oven surfaces by convection was 1.10 kW through the Churchill and Churchill (1975) correlation. This confirmed that radiative heat fluxes could be neglected since heat transfer from the external surfaces was dominated by natural convection.

## Mass Flowrate of Air Exiting the Oven Top Vent

During ‘normal’ operation, the oven consumed  $\sim 3.8\%$  more energy across the SPTs due to hot air leaving the oven through the top vent. It was observed that the mass flowrate [Table 6] was independent of  $T_{sp}$ ; this was because the increased energy consumption of the oven was directed to the convection heating element instead of to the ventilation fan.

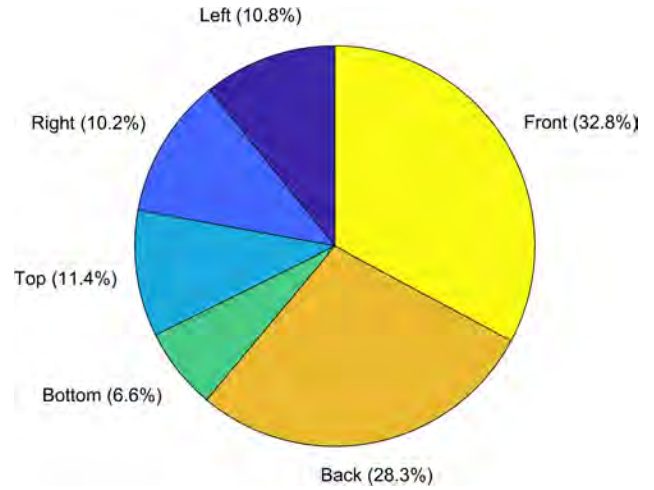


**Figure 12:** Pie chart of the components of energy loss in Phase 1 runs

**Table 6:** Mass flowrate through the oven top vent

| $T_{sp}$ ( $^\circ\text{C}$ ) | $\dot{M}_2^*$ ( $\times 10^{-4}$ kg s $^{-1}$ ) |
|-------------------------------|-------------------------------------------------|
| 160                           | $1.91 \pm 0.02$                                 |
| 200                           | $1.92 \pm 0.02$                                 |
| 240                           | $1.89 \pm 0.02$                                 |

## 4.2 Phase 2

### System Behaviour

Once the cooler unit was attached to the oven (at  $\sim 4500$  s), the oven outlet temperature increased almost instantaneously from  $104^\circ\text{C}$  to reach a new steady state value of  $\sim 160^\circ\text{C}$  (for a run with  $T_{sp} = 160^\circ\text{C}$ ) [see Figure 13a]. The transient behaviour of the heating of the oven-cooler unit connection and the cooler unit took longer, however, both the temperatures of the tubing and the air entering the cooler unit reached steady state within the ‘cooking’ period. Additionally, temperatures within the cooler unit including the water charge increased at a uniform rate [see Figure 13b], indicating steady heat transfer.

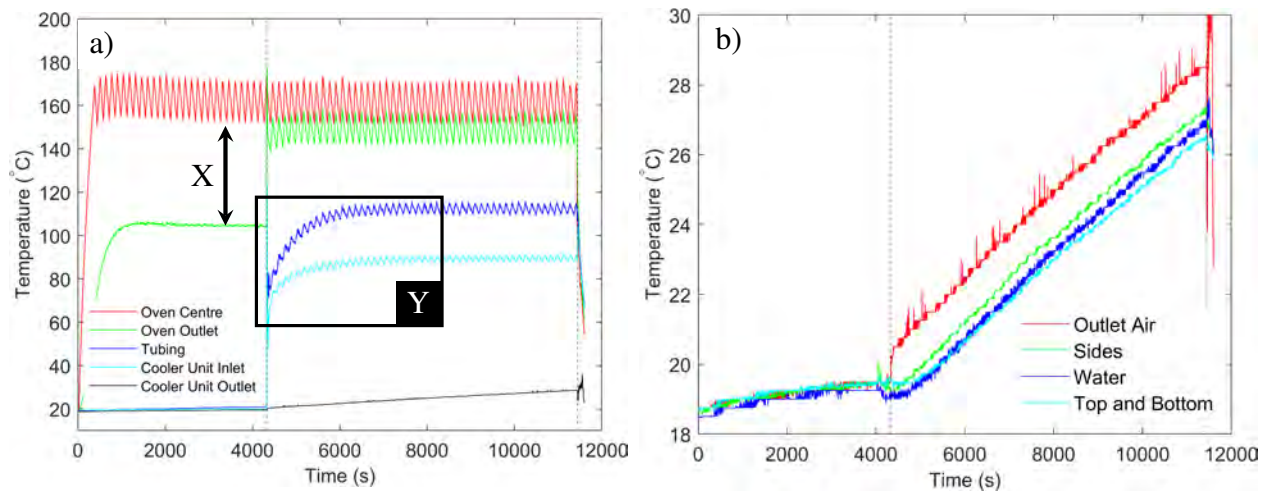


**Figure 13:** Thermal history plots of a Phase 2 run with  $T_{sp} = 160^\circ\text{C}$  (a) along the flow path and (b) in the cooler unit. The oven outlet temperature difference after the cooler unit was attached is labelled  $X$  and the transient behaviour of the heating of the tubing and the cooler unit is labelled  $Y$ . The ‘cooking’ period is indicated by the dashed lines.

The sudden jump in the oven outlet temperature occurred because the measurement was done at the end of the copper tubing; the air within the tubing was stagnant before the cooler unit was brought online. This meant that hot circulated air was not able to access that part of the apparatus. However, the observed temperature was not at ambient due to the conduction of heat through air, which can be seen by comparing the oven outlet THP with that of air in the centre of the oven; the latter had clear cyclic behaviour representing the OOC dynamics which circulated through forced convection, but the former did not. When the bung and sealing were removed and air flowed into the cooler unit, the main mode of heat transfer to air at the oven outlet was forced convection as observed by the cyclic OOC behaviour.

During the ‘cooking’ period, temperatures recorded at locations further away from the centre of the oven were cooler, with smaller OOC amplitudes but with the same frequency. This indicated that

heat transfer through the length of the tubing of the cooler unit was not rate limited (by conduction through air) because it was dominated by forced convection from the ventilation fan. This also indicated that heat was lost through the flow path; in fact, the air entering the cooler unit had lost more than half of its thermal energy relative to ambient from the oven through the insulated tubing. Despite the large differences between the temperatures of the air at the cooler unit inlet and outlet ( $\sim 60$  K difference), the cooler unit and its water charge had similar temperatures and increased at the same rate as well. For the aluminium frame, this was because of its high thermal conductivity,<sup>26</sup> however for the water, this indicated the presence of convection currents.

### Mass Flowrate of Air Exiting the Cooler Unit

Table 7 summarises the mass flowrates of air exiting the cooler unit for each SPT. As  $T_{sp}$  increased, the viscosity of air increased, and the decreasing Reynolds numbers indicated greater frictional losses to the walls of the tubing, leading to the reduction of flowrates.

**Table 7:** *Mass flowrate through the cooler unit*

| $T_{sp}$ (°C) | $\dot{M}_5$ ( $\times 10^{-4}$ kg s $^{-1}$ ) | Reynolds Number |
|---------------|-----------------------------------------------|-----------------|
| 160           | $1.59 \pm 0.02$                               | 478             |
| 200           | $1.47 \pm 0.01$                               | 430             |
| 240           | $1.30 \pm 0.01$                               | 363             |

These mass flowrates were similar to those calculated exiting the oven vent [refer to Table 6] and indicated that the outlet made at the back of the oven for the cooler unit roughly mimics that of the oven vent.

### Energy Balance

The relative proportions of heat transfer were consistent across the SPTs. Although 98% of the input energy was lost through conduction across the oven walls and door, it was expected that this proportion significantly reduces when the oven is ‘cooking’ a food item. Heat transfer to the cooler unit water accounted for most of the remaining 2%, with  $\eta_r = 1.4\%$  indicating the ability of the cooler unit to recover energy.

There are several ways  $\eta_r$  could be improved. One is to use thicker insulation for the oven-cooler unit connection. Assuming that the connection can be made short enough that heat loss through the tubing becomes negligible, calculations indicate that  $\eta_r$  would only improve by 0.4% (which is considered negligible when considering the overall system). Since the majority of heat loss was through the oven walls and door, efforts should focus towards improving oven insulation instead.

### 4.3 Phase 3

#### Pseudo-Chicken

The final trial and error iteration of the pseudo-chicken which *just* evaporated all the 200 g charge of water in 4800 s had the following design [see Figure 14a]:

- a Pyrex<sup>®</sup> tray container (1429 g) with 200 g water
- two pieces of aluminium kitchen foil<sup>ii</sup> (55.0 × 35.0 cm) wrapped around the container
- a kitchen foil lid (55.0 × 35.0 cm) with an 8 × 10 array of 7.0 mm diameter perforations

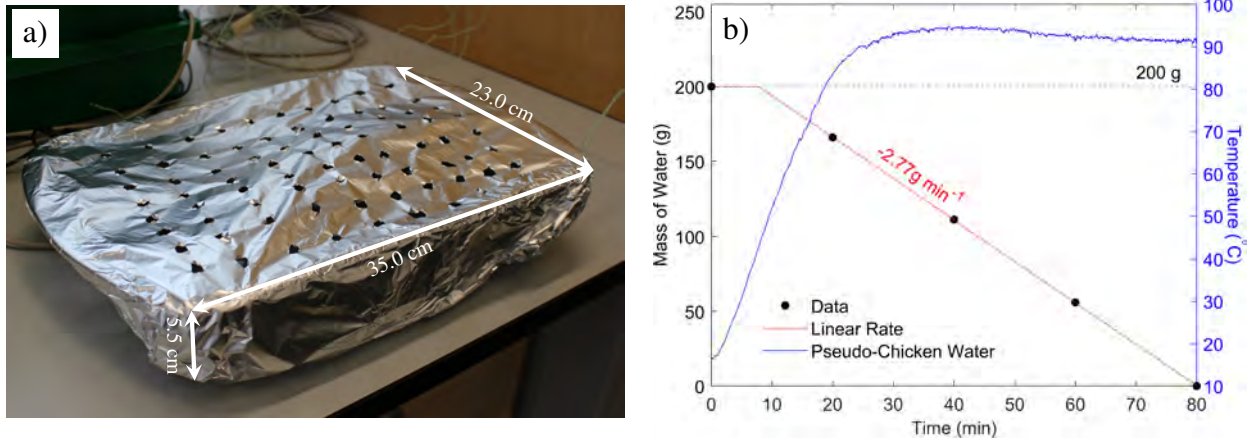


**Figure 14:** (a) The final pseudo-chicken design. (b) Evaporation rate plot (red) and temperature (blue) of the water in the pseudo-chicken.

The final design was confirmed through monitoring the evaporation rate by weighing the pseudo-chicken after different ‘cooking’ periods. The ERP in Figure 14b showed that the water evaporated at a uniform (linear) rate after an initial transient. It was assumed that no water was lost through this period until its temperature reached  $T_{boil,w}$ . This linear behaviour has also been observed in studies using HIPOR bricks, further validating the use of the pseudo-chicken.<sup>2</sup> The ERP also helped fine-tune the design of the pseudo-chicken, as a whole raw chicken evaporates 200 g of water in 80 min, which is equivalent to observing the linear rate pass through (80,0) on the ERP. The measured temperature transient state of the water in the cooler unit ( $\sim 27$  min) was longer than the measured evaporation rate transient behaviour ( $\sim 8$  min). This mismatch came from the ERP assumption that water loss only occurred when the water temperature reached  $T_{boil,w}$ . In reality  $T_{boil,w}$  was never reached and water would have started evaporating as soon as it was placed in the oven, at an increasing rate as it heated up. Hence, distinct heating and evaporation stages could not be identified as they occurred simultaneously; instead, the transition to the linear evaporation rate was gradual and occurred before the pseudo-chicken water temperature reached 95°C.

<sup>ii</sup>Kitchen foil has a thermal conductivity 200× larger than Pyrex<sup>®</sup>.<sup>26</sup> its purpose was not to resist heat transfer, but to give the pseudo-chicken a uniform outer layer in terms of material properties.



## System Behaviour

After the pseudo-chicken was placed in the oven, the temperatures within the oven cavity reached a new steady state [see Figure 15a]. With  $T_{sp} = 200^{\circ}\text{C}$ , the average difference in steady state temperatures for this transition was  $-13\text{ K}$ , indicating that the pseudo-chicken was consuming a considerable amount of energy through sensible heating and water evaporation.

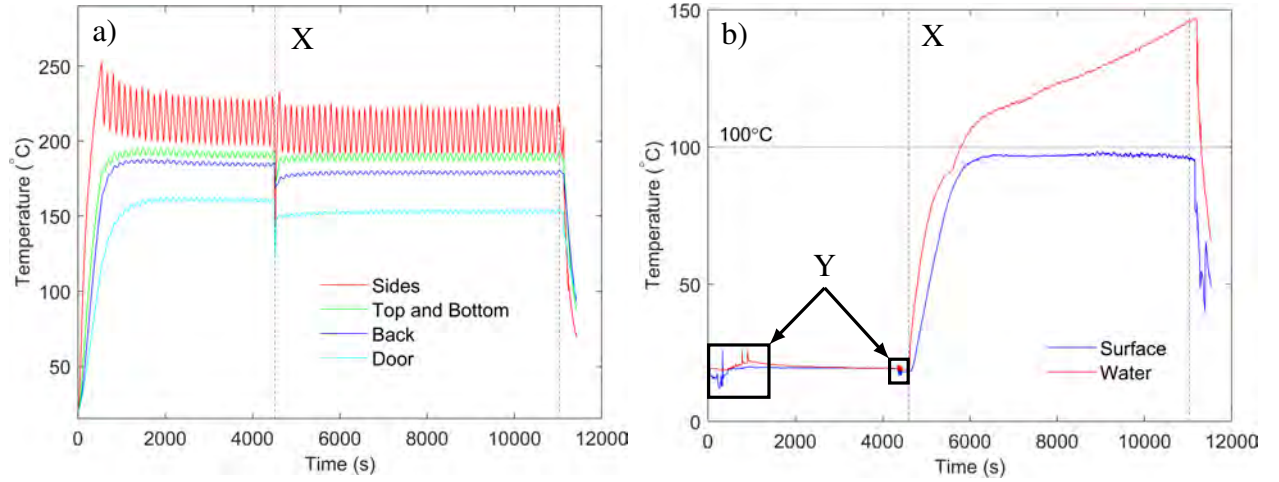


**Figure 15:** Thermal history plots of a Phase 3 run with  $T_{sp} = 200^{\circ}\text{C}$  (a) inside the oven and (b) of the pseudo-chicken. The time at which the pseudo-chicken was added is labelled **X** and the temperature fluctuations due to thermocouple short circuiting from thermocouple placement in preparation for the run are labelled **Y**. The ‘cooking’ period is indicated by the dashed lines.

Temperature fluctuations were observed when using the pseudo-chicken and was a result of thermocouple short circuiting [see Figure 15b]. Since the thermocouple measuring the pseudo-chicken surface was in contact with the kitchen foil, and the thermocouple measuring the water temperature was in contact with the water, the signals sent through the latter (which was done before the former thermocouple due the signal processing order) conducted through the water and through the kitchen foil to reach the former thermocouple, creating an undesired connection between the two and short circuiting the measurements. These issues were corrected by insulating the water thermocouple completely with Kapton tape.

From the shape of the THPs of the pseudo-chicken surface and water in Figure 15b, it can be seen that both of these heated up under similar heat transfer mechanisms (conduction). Although it was expected that water in the pseudo-chicken would reach its boiling point of  $100^{\circ}\text{C}$ , a temperature of  $95^{\circ}\text{C}$  was measured. This confirmed that water loss was a result of evaporation instead of boiling, indicating that the rate of evaporation was phase change limited as it was governed by the rate of heat transferred to the pseudo-chicken.



## Energy Balance

Over  $\sim 7500$  s of ‘cooking’ with  $T_{sp} = 200^\circ\text{C}$ , the pseudo-chicken consumed 15.8% of the energy supplied to the oven, which is a typical  $\eta_c$  value for domestic ovens. Higher  $\eta_c$  values can be achieved by (again) better insulation due to the reduction in heat loss from the oven walls. Additionally, during ‘normal’ operation with the pseudo-chicken, the oven consumed  $\sim 4.0\%$  more energy across the SPTs due to hot air leaving the oven through the top vent.

## 4.4 Phase 4

### Energy Balance and Efficiencies

Similarities in the effective powers ( $P_{eff,j}$ ) [see Table 8<sup>iii</sup>] of experiments in Phases 3 (with ‘normal’ operation) and 4 further showed that the outlet made at the back of the oven for the cooler unit mimicked that of the oven top vent. These were calculated by dividing the total energy supplied to the oven within the ‘cooking stage’ by its duration.

**Table 8:** Effective power supplied to the oven during the ‘cooking’ stages in Phases 3 and 4

| $T_{sp}$ ( $^\circ\text{C}$ ) | $P_{eff,3}$ (kW) | $P_{eff,3}^*$ (kW) | $P_{eff,4}$ (kW) |
|-------------------------------|------------------|--------------------|------------------|
| 160                           | 0.78             | 0.81               | 0.81             |
| 200                           | 1.04             | 1.08               | 1.06             |
| 240                           | 1.29             | 1.34               | 1.32             |

Across the SPTs, the oven cooking efficiency [Table 9] was between 15.6 – 17.2% and the cooler unit consistently increased  $\eta_c$  by 1.0%, bringing the total oven efficiency to 16.6 – 18.2%.

**Table 9:** Efficiencies in Phase 4 runs. Oven cooking efficiencies in Phase 3 runs are in [square brackets] and cooler unit efficiencies in Phase 2 runs are in {braces}.

| $T_{sp}$ ( $^\circ\text{C}$ ) | $E_{cooking}$ (MJ) | $E_{recovered}$ (MJ) | $E_{lost} + E_{cooking} + E_{recovered}$ (MJ) | $\eta_c$ (%) | $\eta_r$ (%) | $\eta_T$ (%) |
|-------------------------------|--------------------|----------------------|-----------------------------------------------|--------------|--------------|--------------|
| 160                           | 0.94               | 0.06                 | 6.04                                          | 15.6 [14.9]  | 1.0 {1.3}    | 16.6         |
| 200                           | 1.26               | 0.08                 | 7.60                                          | 16.6 [15.8]  | 1.0 {1.2}    | 17.6         |
| 240                           | 1.55               | 0.09                 | 9.03                                          | 17.2 [16.5]  | 1.0 {1.2}    | 18.2         |

The  $\eta_r$  values in Phase 2 were higher than in Phase 4 because the pseudo-chicken consumed a considerable proportion of the energy supplied to the oven. In Phase 4, the temperature of the air entering the cooler unit was consistently 2 – 3 K lower than in Phase 2 [see Figure 16], so the cooler unit recovered less thermal energy overall.

The  $\eta_c$  values in Phase 3 were lower than in Phase 4 because the pseudo-chicken had lower rates

<sup>iii</sup>Since the batch calculations for each run had different timescales (due to the slight differences in the frequencies of the OOC), direct energy comparisons could not be made and so comparisons of the effective power were done instead.

of heat transfer from the lack of the cooler unit attachment. With similar OOC amplitudes in the temperature, the average time period of OOC in Phase 3 (146 s) was 18 s longer than in Phase 4 (128 s). This indicated that less energy was supplied to the oven and hence to the pseudo-chicken [Figure 17], decreasing  $\eta_c$ . On the other hand, the  $\eta_c$  values in Phase 3 runs under ‘normal’ operation (with the oven top vent open) were similar to those in Phase 4 due to the similar mass flowrates of air exiting the oven, allowing for the use of  $\eta_c$  values from Phase 4 as the benchmark for ‘normal’ operation.

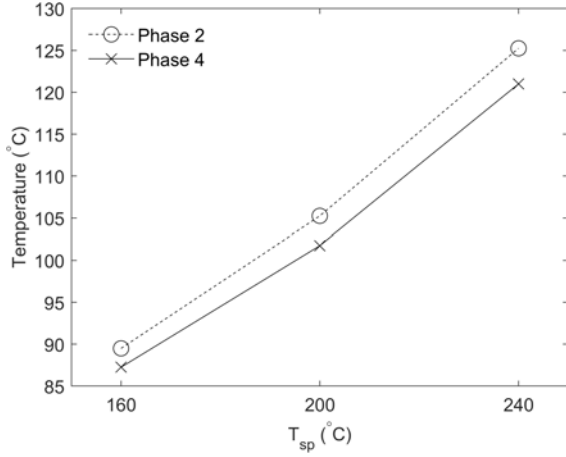


**Figure 16:** Air temperatures at the cooler unit inlet for Phases 2 and 4 at steady state during the ‘cooking’ period

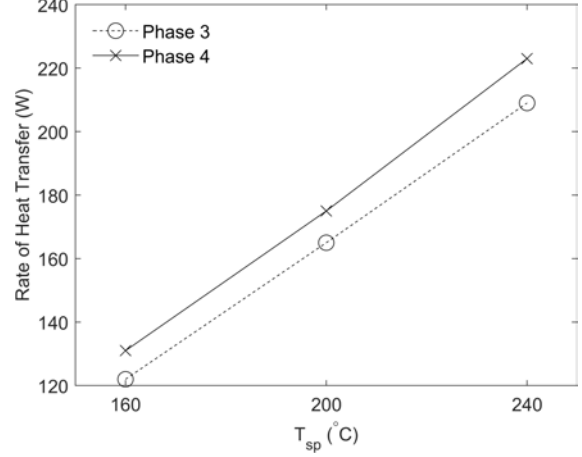


**Figure 17:** Rate of heat transfer to the pseudo-chicken for Phases 3 and 4 at steady state during the ‘cooking’ period

### Cooler Unit Heat Exchanger Performance

Across the SPTs, the duty of the cooler unit was 11.4 – 14.4 W, giving  $(UAF)_{duty} = 0.27 \pm 0.01 \text{ W K}^{-1}$  whilst the rate of heat transfer to the cooler unit water gave  $(UAF)_{cu,w} = 0.25 \pm 0.04 \text{ W K}^{-1}$ . The similarity in these two values showed that the two heat exchanger models were consistent with each other. Additionally, the small surface area for heat transfer in the cooler tubes ( $\sim 2.2 \times 10^{-4} \text{ m}^2$ ) gave  $UF$  values of  $\sim 1200 \text{ W m}^{-2} \text{ K}^{-1}$ . This was within the range of typical  $U$  values ( $700 - 1500 \text{ W m}^{-2} \text{ K}^{-1}$ ) for shell and tube heat exchangers with aqueous and organic vapours as the ‘hot fluid’ and water as the ‘cold fluid’,<sup>27</sup> further showing that the cooler unit performed well as a heat exchanger and could even be modelled as one.

### Cooler Unit Air Exit Temperature

The temperatures of the air exiting the cooler unit and the water within the cooler unit heated up at similar rates [see Figure 18]. The former started at ambient temperatures of  $\sim 20.5^\circ\text{C}$  whereas the latter started at temperatures of  $\sim 19.5^\circ\text{C}$ . The water was consistently 1 – 2 K below the air at the outlet, indicating that heat transfer was in the direction towards the water throughout the entire

length of the cooler tubes. The highest temperature observed for the air leaving the cooler unit was 30°C for a run with  $T_{sp} = 240^\circ\text{C}$ . This suggested that a larger heat transfer surface area for the cooler tubes and / or a larger water charge would be required to limit the value below 30°C so that the cooler unit temperature does not pose a problem for handling.

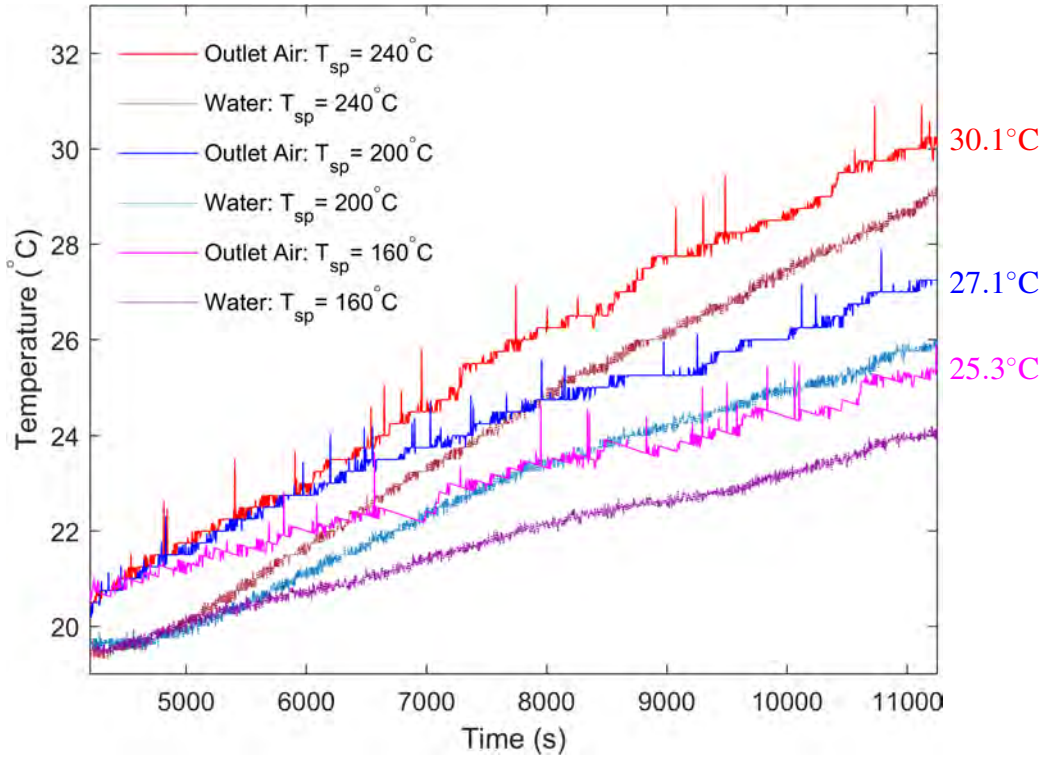


**Figure 18:** Thermal history plot of the outlet air and the water of the cooler unit for Phase 4 runs

Depending on the recipe, cooking oils and / or fats may be found in the food item. The majority of cooking oils and fats have reported to have  $T_{boil} > 100^\circ\text{C}$ ,<sup>28</sup> however, their dew points when mixed with water vapour have not been readily reported. Fortunately, there have been a few studies that have cooked food items such as ground meat,<sup>29</sup> chicken nuggets<sup>30</sup> and chicken fillets<sup>31</sup> in ovens with  $T_{sp} = 170 - 180^\circ\text{C}$ . These have indicated that the dew points of lipid-water vapour mixtures within the oven cavity are between 90 – 110°C, showing that the volatile lipids within the cooler unit would be theoretically removed from the vented gases.

A source of concern however lies with the lipid melting points. Most cooking oils have melting points below  $-5^\circ\text{C}$ ; however, due to their higher degree of saturation, the melting points of fats lie around room temperature.<sup>32</sup> For example, butter melts between 32 – 35°C, indicating that if a recipe for a food item calls for the use of butter, it would condense and solidify within the cooler unit when operated with the SPTs used in this project. Therefore, the cooler unit needs to be designed to remove fats as they will foul the cooler unit, for example, with a slope to drain fats when they are still molten.

## 4.5 Proposals for Further Work

Due to the limited timeframe and availability of material, the system apparatus used in this research project was not optimised. Several improvements and modifications can be made in the future to limit heat loss to the environment.

### Oven

Most of the heat lost from the system apparatus was by conduction through the oven walls and door. In Phase 4 experiments, this accounted for 83% of the total amount of heat transferred, clearly indicating that improved insulation is needed (as well as the original door arrangement which is estimated to reduce electrical energy consumption in this research project by  $\sim 10\%$ ). Studies have shown that small modifications can make noticeable energy savings, for example using glass wool to insulate the outer surface of the oven walls ( $-7.7\%$  in energy consumption) and using aluminium self-adhesive insulating tape to seal the oven door and several slits and gaps on the oven ( $-12.6\%$  in energy consumption).<sup>12</sup> Further work on the implications these modifications have for the cooler unit and the effect on  $\eta_c$  should be done.

### Oven-Cooler Unit Connection

By the time the hot air entered the cooler unit, it had lost more than half of its thermal energy relative to ambient through the tubing. A shorter connection and thicker insulation should be used for further experiments. In the oven prototype currently used by CSI, the connections to the oven cavity can be half the length of that used in this project. This can be done by connecting them through the top surface of the oven cavity, further utilising the oven wall insulation as well. Proper tubing insulation should also be used (instead of makeshift ones using nitrile rubber insulation sheets) to ensure that the resistance to heat transfer is axially uniform.

### Cooler Unit

The cooler unit used in this research project was the first prototype from CSI. Although it recovered a noticeable proportion of energy ( $\eta_r = 1.0\%$ ) and reached cool enough temperatures to theoretically condense volatile lipids, an optimal cooler unit design would aim for better energy recovery and for the ability to remove solid fat deposits as well.

The cooler unit lost a small amount of heat during operation through heat conduction across its surfaces and so although insulation can be incorporated onto the unit, removing the need for external insulation, this would not significantly improve heat recovery. Mixtures of oil and water can also be used to characterise fluids found in typical food items, giving an accurate idea of the ability

of the cooler unit to operate as intended.

Although the cooler unit was able to recover energy in the form of heated water, this water must be used to justify its ability. Experiments should be done to determine whether the intended use of the heated water at 30°C (for common household chores *e.g.* washing dishes or doing laundry) can realise energy savings.

### Pseudo-Chicken

As mentioned in Section 1.2, measurements of oven efficiency are currently done under European Standard EN 60350-1:2016/A1:2021 using HIPOR bricks saturated with moisture. These are ceramic bricks that are made with defined specifications from the standard and even have specifically drilled holes for thermocouples to sit in.

Although limitations of the research project meant that pseudo-chickens had to be used, HIPOR bricks should be used in the future to perform more accurate and representative experiments of common food items. Additionally, since HIPOR bricks are all standardised, the random error between different bricks will be minimised, as opposed to the use of different pseudo-chickens, which incurred some random error due to the reproducibility in preparing different components required to set them up (kitchen foil pieces and perforation arrays).

## 4.6 Error Analysis

### Phase 1

The small discrepancies of the Phase 1 runs ( $0.1\% < |\delta_{1,\%}| < 0.2\%$ ) from the energy balance [Table 10] suggested high experimental repeatability, showing that the results were consistent, reproducible and were resistant to minor environmental variations such as ambient air and water temperatures.

**Table 10:** *Energy balance from Phase 1 runs*

| $T_{sp}$ (°C) | $P_{av}$ (kW) | $Q_{lost,oven}$ (kW) | $\delta_1$ (kW) | $\delta_{1,\%}$ (%) |
|---------------|---------------|----------------------|-----------------|---------------------|
| 160           | 0.71          | 0.72                 | −0.01           | −0.1                |
| 200           | 0.89          | 0.90                 | −0.01           | −0.1                |
| 240           | 1.12          | 1.09                 | +0.03           | +0.2                |

### Phase 2

The small discrepancies of the Phase 2 runs ( $0.6\% < \delta_{2,\%} < 1.1\%$ ) suggested that all energy losses present were accounted for [see Table 11]. The consistent magnitude of the discrepancies indicated the presence of systematic errors; however, potential sources including measurement inaccuracies

of the air temperature (since it took a small amount of time to heat up / cool down the suspended thermocouples) were considered negligible for the purposes of this study (due to the timescales over which the batch calculations were performed).

**Table 11:** *Energy balance of Phase 2 runs*

| $T_{sp}$ (°C) | $E_T$ (MJ) | $E_{lost} + E_{recovered}$ (MJ) | $\delta_2$ (MJ) | $\delta_{2,\%}$ (%) |
|---------------|------------|---------------------------------|-----------------|---------------------|
| 160           | 5.30       | 5.24                            | +0.06           | +1.4                |
| 200           | 6.97       | 6.91                            | +0.06           | +0.9                |
| 240           | 8.04       | 7.99                            | +0.05           | +0.6                |

### Phase 3

The small discrepancies of the Phase 3 runs ( $0.5\% < \delta_{3,\%} < 1.5\%$ ) suggested that the only energy losses present was through the oven walls and door [see Table 12]. The discrepancies for Phase 3 runs were more random than Phase 2, however since they were all  $> 0$ , both random and systematic errors were likely to have affected the results. Random errors in the system apparatus included the construction of the pseudo-chicken, as well as the variability of the  $T_{sp}$  as a result of the oven settings. Since the  $T_{sp}$  was set by a 3.0 cm knob (OD), it was difficult to ensure that it was set to the same position for every run.

**Table 12:** *Energy balance of Phase 3 runs*

| $T_{sp}$ (°C) | $E_T$ (MJ) | $E_{lost,oven} + E_{cooking}$ (MJ) | $\delta_3$ (MJ) | $\delta_{3,\%}$ (%) |
|---------------|------------|------------------------------------|-----------------|---------------------|
| 160           | 6.27       | 6.20                               | +0.07           | +1.1                |
| 200           | 8.83       | 8.79                               | +0.04           | +0.5                |
| 240           | 9.55       | 9.40                               | +0.14           | +1.5                |

### Phase 4

The values of the discrepancies in Phase 4 runs ( $1.6\% < \delta_{4,\%} < 3.8\%$ ) were small [see Table 13], suggesting that all the sources of heat loss and transfer were accounted for; however, they were larger both proportionately and by value than in Phases 2 and 3. The discrepancies were also more random than those in Phase 3, but since they were all  $> 0$ , both random and systematic errors were once again likely to have affected the results.

**Table 13:** *Energy balance of Phase 4 runs*

| $T_{sp}$ (°C) | $E_T$ (MJ) | $E_{lost} + E_{recovered} + E_{cooking}$ (MJ) | $\delta_4$ (MJ) | $\delta_{4,\%}$ (%) |
|---------------|------------|-----------------------------------------------|-----------------|---------------------|
| 160           | 6.28       | 6.04                                          | +0.24           | +3.8                |
| 200           | 7.77       | 7.60                                          | +0.17           | +2.2                |
| 240           | 9.17       | 9.03                                          | +0.14           | +1.6                |

Additional sources of random errors came from inconsistent placement of the pseudo-chicken in

the oven. To minimise the amount of heat lost when entering the ‘cooking’ stage, the pseudo-chicken was quickly placed on the tray in the oven, without much time spent on perfecting its placement. This could have led to slightly different positions of the pseudo-chicken for each run which would have given different rates of heating and hence different  $E_{cooking}$ s for the pseudo-chicken [see Table 14].

**Table 14:** *Distributions of  $E_{cooking}$  values*

| $T_{sp}$ (°C) | $E_{cooking}$ (MJ) |      |      |
|---------------|--------------------|------|------|
| 160           | 0.95               | 0.93 | 0.94 |
| 200           | 1.27               | 1.25 | 1.24 |
| 240           | 1.49               | 1.58 | 1.52 |



## 5 Conclusions

The oven and cooler unit apparatuses were constructed, connected together and commissioned. The system was fully characterised by solving for four different parameters to ensure that all sources of heat transfer were accounted for.  $U_5$  was solved for using an inverse problem with the energy balances for the empty oven; its value ( $10.4 \text{ W m}^{-2} \text{ K}^{-1}$ ) was further verified through comparison with values obtained by Cernela *et al.* (2013) ( $11.6 \text{ W m}^{-2} \text{ K}^{-1}$ ).  $\dot{M}_2^*$  was calculated at  $1.91 \times 10^{-4} \text{ kg s}^{-1}$  by using a simple sensible heat change calculation.  $\dot{M}_5$  was measured between  $1.30 \times 10^{-4} - 1.59 \times 10^{-4} \text{ kg s}^{-1}$  using a bubble flowmeter connected to the outlet of the cooler unit. This flowrate was observed to decrease at higher temperatures due to the increased frictional losses in the tubing. Lastly, the food item was designed through trial and error by benchmarking its performance with that of raw chicken. The final design was constructed from a Pyrex<sup>®</sup> tray and kitchen foil with perforations on the top layer; the number and sizes of these perforations were further fine-tuned using trends in the evaporation rate of the water charge.

The temperature of the air exiting the cooler unit reached at most  $30^\circ\text{C}$  (from a  $T_{sp} = 240^\circ\text{C}$ ) which was lower than the dew points of lipid-water vapour mixtures ( $90 - 110^\circ\text{C}$ ) reported from various studies that cooked common food items in ovens. Additionally, heat transfer within the cooler unit was shown to be dominated by forced convection as seen by the cyclic OOC behaviour, verifying the ability of the cooler unit to theoretically condense out volatile cooking oils and fats.

During ‘normal’ operation, the oven cooking efficiency was between  $15.6 - 17.2\%$ . When the cooler unit was attached, an additional  $1.0\%$  of the energy consumed was recovered, increasing the total oven efficiency to  $16.6 - 18.2\%$ . The cooler unit was also observed to perform similar to that of a heat exchanger with an overall heat transfer coefficient value of  $\sim 1200 \text{ W m}^{-2} \text{ K}^{-1}$ . This was further verified through comparison with typical  $U$  values for shell and tube heat exchangers found from the literature ( $700 - 1500 \text{ W m}^{-2} \text{ K}^{-1}$ ), indicating the applicability of heat exchanger models to the cooler unit.

Overall, this research project has fulfilled its purpose in demonstrating that the Cambridge Sensor Innovation cooler unit is suitable for cleaning vented oven gases and can also act as an energy recovery unit, provided that the thermal energy within the cooler unit water is fully utilised (*e.g.* for household chores).

## References

- [1] Prime Appliance Repairs, 2021. “*Types of Ovens and Which Is Best for You?*” [Accessed 1 April 2022]. URL: <https://primeappliancerepairs.com/blog/types-of-ovens-and-which-is-best-for-you>.
- [2] O. Isik et al. (2013). Investigation of different wall profiles on energy consumption and baking time in domestic ovens. In: *EPJ Web of Conferences* **45** (Apr. 2013), pp. 01044–. DOI: 10.1051/epjconf/20134501044.
- [3] LG Help Library, 2021. “*Convection cooking, baking, roasting – Oven heating elements*”. [Accessed 1 April 2022]. URL: [https://www.lg.com/ca\\_en/support/product-help/CT20098053-20150887756385](https://www.lg.com/ca_en/support/product-help/CT20098053-20150887756385).
- [4] Bob Vila, 2021. “*Solved! What is a Convection Oven?*” [Accessed 1 April 2022]. URL: <https://www.bobvila.com/articles/what-is-a-convection-oven>.
- [5] Emine Doğru Bolat, Kadir Erkan, and Seda Postalcioglu (2005). *Microcontroller based temperature control of oven using different kinds of autotuning PID methods*. In: *Australasian Joint Conference on Artificial Intelligence*. Springer. Dec. 2005, pp. 1295–1300.
- [6] R. Rodríguez Quintero et al. (2020). *Review study of Ecodesign and Energy Labelling for Cooking appliances*. URL: [https://susproc.jrc.ec.europa.eu/product-bureau/sites/default/files/2020-07/CA\\_\%20Prep\%20Study\\_draft1\\_Feb2020.pdf](https://susproc.jrc.ec.europa.eu/product-bureau/sites/default/files/2020-07/CA_\%20Prep\%20Study_draft1_Feb2020.pdf).
- [7] Anibal De Almeida et al. (2011). Characterization of the household electricity consumption in the EU, potential energy savings and specific policy recommendations. In: *Energy and buildings* **43.8** (Aug. 2011), pp. 1884–1894.
- [8] ITEH Standards, 2021. “*EN 60350-1:2016/A1:2021*”. [Accessed 1 April 2022]. URL: <https://standards.iteh.ai/catalog/standards/clc/a2af7375-ff30-4bed-90e7-8219b8b3ee77/en-60350-1-2016-a1-2021>.
- [9] Statista, 2021. “*UK: household electricity prices 2020*”. [Accessed 1 April 2022]. URL: <https://www.statista.com/statistics/418126/electricity-prices-for-households-in-the-uk>.
- [10] United States Environmental Protection Agency, 2021. “*Sources of Greenhouse Gas Emissions*”. [Accessed 1 April 2022]. URL: <https://www.epa.gov/ghgemissions/sources-greenhouse-gas-emissions>.
- [11] Michelle Putter, 2021. “*Saving electricity in the office*”. [Accessed 1 April 2022]. URL: <https://cpdonline.co.uk/knowledge-base/health-and-safety/saving-electricity-in-the-office>.
- [12] M Penssek et al. (2005). Energy consumption analysis of domestic oven. In: *Strojniski Vestnik/Journal of Mechanical Engineering* **51** (Jan. 2005), pp. 405–410. DOI: 10.1615/ICHMT.2004.IntThermSciSemin.560.
- [13] Fabio Burlon (2015). Energy Efficiency of Combined Ovens. In: *Energy Procedia* **82** (Dec. 2015), pp. 986–993. DOI: 10.1016/j.egypro.2015.11.856.
- [14] Cambridge Oven Innovation, 2022. [Accessed 1 April 2022]. URL: <https://www.camoven.com>.
- [15] DuPont, 2019. “*DuPont™ Kapton® HN - Polyimide Film*”. [Accessed 1 April 2022]. URL: <https://www.dupont.com/content/dam/dupont/amer/us/en/products/ei-transformation/documents/DEC-Kapton-HN-datasheet.pdf>.
- [16] NEFF. “*Built-in oven Stainless steel oven B12S32N3GB*”. [Accessed 1 April 2022]. URL: <https://www.neff-home.com/uk/productlist/B12S32N3GB#/Togglebox=accessories/Togglebox=manuals/Togglebox=accessoriesOthers>.

- [17] University of Cambridge, Department of Chemical Engineering and Biotechnology. “*Chemical Engineering Tripos Part IIB Syllabus 2021-22*”. [Accessed 1 April 2022].
- [18] Maurizio Vannoni et al. (2013). Measuring the thickness of soap bubbles with phase-shift interferometry. In: *Optics express* **21** (Aug. 2013), pp. 19657–19667. DOI: 10.1364/OE.21.019657.
- [19] Spehro Pefhany, 2021. “*Why do consumer ovens use thermostats instead of PID + PWM?*” [Accessed 1 April 2022]. URL: <https://electronics.stackexchange.com/questions/554441/why-do-consumer-ovens-use-thermostats-instead-of-pid-pwm>.
- [20] R.H.S. Winterton (1997). *Heat Transfer*. Oxford chemistry primers. Oxford University Press. ISBN: 9785751000332.
- [21] Seong Hyun Park et al. (2018). Numerical study on the effect of different hole locations in the fan case on the thermal performance inside a gas oven range. In: *Applied Thermal Engineering* **137** (Mar. 2018). DOI: 10.1016/j.applthermaleng.2018.03.087.
- [22] RS Components. “*Black Nitrile Rubber Tank Insulation, 2m × 500mm × 13mm*”. [Accessed 1 April 2022]. URL: <https://uk.rs-online.com/web/p/thermal-insulation/0486029>.
- [23] Fluke Process Instruments, 2021. “*Emmissivity - Metals*”. [Accessed 1 April 2022]. URL: <https://www.flukeprocessinstruments.com/en-us/service-and-support/knowledge-center/infrared-technology/emissivity-metals>.
- [24] Stuart Churchill and Renate Churchill (1975). Comprehensive Correlating Equation for Heat and Component Transfer by Free Convection. In: *AIChE Journal* **21** (May 1975), pp. 604–606. DOI: 10.1002/aic.690210330.
- [25] Jérémie Cernela, Bertrand Heyd, and Bertrand Broyart (2014). Evaluation of heating performances and associated variability of domestic cooking appliances (oven-baking and pan-frying). In: *Applied Thermal Engineering* **62** (Jan. 2014), pp. 758–765. DOI: 10.1016/j.applthermaleng.2013.08.045.
- [26] Engineering Tool Box, 2021. “*Solids, Liquids and Gases - Thermal Conductivities*”. [Accessed 1 April 2022]. URL: [https://www.engineeringtoolbox.com/thermal-conductivity-d\\_429.html](https://www.engineeringtoolbox.com/thermal-conductivity-d_429.html).
- [27] R. K. Sinnott (1993). *Chapter 12 - Heat-transfer Equipment*. In: *Coulson and Richardson's Chemical Engineering (Second Edition)*. Ed. by R.K. Sinnott. Second Edition. Chemical Engineering Technical Series. Amsterdam: Pergamon, 1993, pp. 565–702. ISBN: 978-0-08-041865-0. DOI: <https://doi.org/10.1016/B978-0-08-041865-0.50020-9>. URL: <https://www.sciencedirect.com/science/article/pii/B9780080418650500209>.
- [28] Chemical Forums, 2006. “*Boiling point of butter*”. [Accessed 1 April 2022]. URL: <https://www.chemicalforums.com/index.php?topic=6828.0>.
- [29] Mojtaba Zabihinpour et al. (2015). Fuzzy mean and range control charts for monitoring fuzzy quality characteristics: A case study in food industries using chicken nugget. In: *IEEE International Conference on Industrial Engineering and Engineering Management* **2015** (Mar. 2015), pp. 759–763. DOI: 10.1109/IEEM.2014.7058740.
- [30] Mitra C. Tripuraneni (2006). *Fat transport properties and mechanisms during cooking of ground meat*. PhD thesis, p. 164. ISBN: 978-0-542-89945-4.
- [31] Ruud Van der sman (2013). Modeling cooking of chicken meat in industrial tunnel ovens with the Flory-Rehner theory. In: *Meat science* **95** (Mar. 2013). DOI: 10.1016/j.meatsci.2013.03.027.
- [32] VCE Chemistry. “*Fats and oils*”. [Accessed 1 April 2022]. URL: <https://chemistryvce.weebly.com/fats-and-oils.html>.

# Nomenclature

## Roman

|           |                                              |                                  |
|-----------|----------------------------------------------|----------------------------------|
| $A$       | Area for heat transfer                       | $\text{m}^2$                     |
| $C_p$     | Specific heat capacity                       | $\text{J kg}^{-1} \text{K}^{-1}$ |
| $d$       | Thickness                                    | $\text{m}$                       |
| $D$       | Diameter                                     | $\text{m}$                       |
| $E$       | Amount of energy                             | $\text{J}$                       |
| $F$       | Correction factor                            | —                                |
| $g$       | Acceleration due to gravity                  | $9.81 \text{ m s}^{-2}$          |
| $Gr$      | Grashoff number                              | —                                |
| $H$       | Vertical distance                            | $\text{m}$                       |
| $h$       | Heat transfer coefficient                    | $\text{W m}^{-2} \text{K}^{-1}$  |
| $k$       | Thermal conductivity                         | $\text{W m}^{-1} \text{K}^{-1}$  |
| $L$       | Characteristic length                        | $\text{m}$                       |
| $M$       | Amount of mass                               | $\text{kg}$                      |
| $\dot{M}$ | Mass flowrate of air                         | $\text{kg s}^{-1}$               |
| $m$       | Coefficient for Winterton (1998) correlation | —                                |
| $Nu$      | Nusselt number                               | —                                |
| $P$       | Power supplied to oven                       | $\text{W}$                       |
| $Pr$      | Prandtl number                               | —                                |
| $Ra$      | Rayleigh number                              | —                                |
| $\dot{Q}$ | Rate of heat loss                            | $\text{W}$                       |
| $T$       | Temperature                                  | $\text{K}$ or $^{\circ}\text{C}$ |
| $t$       | Time scale                                   | $\text{s}$                       |
| $U$       | Overall heat transfer coefficient            | $\text{W m}^{-2} \text{K}^{-1}$  |
| $X$       | Total length of oven-cooler unit tubing      | $20.0 \text{ cm}$                |
| $x$       | Length scale                                 | $\text{m}$                       |

## Greek

|               |                                      |                      |
|---------------|--------------------------------------|----------------------|
| $\beta$       | Thermal expansion coefficient        | $\text{K}^{-1}$      |
| $\delta$      | Discrepancy                          | $\text{J}$ or —      |
| $\varepsilon$ | Emissivity                           | —                    |
| $\eta$        | Efficiency                           | —                    |
| $\lambda$     | Specific latent heat of vaporisation | $\text{J kg}^{-1}$   |
| $\nu$         | Kinematic viscosity                  | $\text{J s kg}^{-1}$ |
| $\rho$        | Density                              | $\text{kg m}^{-3}$   |

## Superscripts

- \* ‘Normal’ oven operation

## Subscripts (Components / Materials)

|       |             |
|-------|-------------|
| $air$ | Air         |
| $cu$  | Cooler unit |

|               |                                    |
|---------------|------------------------------------|
| <i>glass</i>  | Glass                              |
| <i>oven</i>   | Oven                               |
| <i>pc</i>     | Pseudo-chicken                     |
| <i>py</i>     | Pyrex <sup>®</sup>                 |
| <i>steel</i>  | Steel                              |
| <i>tubing</i> | Oven-cooler unit tubing connection |
| <i>w</i>      | Water                              |
| <i>wool</i>   | Insulation wool                    |

### Subscripts (Technical)

|                  |                                                   |                    |
|------------------|---------------------------------------------------|--------------------|
| <i>ambient</i>   | Ambient (temperature)                             |                    |
| <i>av</i>        | Average (power)                                   |                    |
| <i>boil</i>      | Boiling (point temperature)                       |                    |
| <i>c</i>         | Oven cooking (efficiency)                         |                    |
| <i>centre</i>    | Oven centre (temperature / thermal heat capacity) |                    |
| <i>conv</i>      | Convection (dimensionless groups)                 |                    |
| <i>cooking</i>   | Cooking (energy)                                  |                    |
| <i>duty</i>      | Duty of the apparatus                             |                    |
| <i>E</i>         | Energy (discrepancy)                              |                    |
| <i>eff</i>       | Effective (power)                                 |                    |
| <i>ex</i>        | External surface of a wall                        |                    |
| <i>f</i>         | Finish / final (time / mass / temperature)        |                    |
| <i>lm</i>        | Log mean (temperature difference)                 |                    |
| <i>lost</i>      | (Energy) lost to surroundings                     |                    |
| <i>mid</i>       | Middle component                                  |                    |
| <i>i</i>         | Surface number                                    | $i \in \{1 - 13\}$ |
| <i>in</i>        | Internal surface of a wall                        |                    |
| <i>inlet</i>     | Inlet of the apparatus                            |                    |
| <i>j</i>         | Experimental phase number                         | $j \in \{1 - 4\}$  |
| <i>outlet</i>    | Outlet of the apparatus                           |                    |
| <i>P</i>         | Power (discrepancy)                               |                    |
| <i>r</i>         | Recovered (efficiency)                            |                    |
| <i>recovered</i> | Recovered (energy)                                |                    |
| <i>s</i>         | Start / initial (time / mass / temperature)       |                    |
| <i>sp</i>        | Set point                                         |                    |
| <i>T</i>         | Total (input energy / efficiency)                 |                    |
| <i>%</i>         | Percentage (discrepancy)                          |                    |

### Abbreviations

|       |                                   |
|-------|-----------------------------------|
| CEP   | Cumulative energy plot            |
| CSI   | Cambridge Sensor Innovation       |
| EFCO  | Electric fan convection oven      |
| ERP   | Evaporation rate plot             |
| HIPOR | High porosity                     |
| OD    | Outer diameter                    |
| OOC   | ON-OFF control                    |
| SPT   | Set point temperature             |
| TEFCO | True electric fan convection oven |
| THP   | Thermal history plot              |

# Appendix

## Programs Used

The programs used to acquire and process the data can be found in the following git repository:  
<https://github.com/codykwok/CETIIBResearchProject.git>.

### Data Measurement Python Program

The program used to measure the energy consumption and temperatures of the system apparatus was previously written by Dr. Jamie Davidson in Python. This program was run on a desktop PC which was connected to the data logger. At the end of each run, the program wrote a .csv file to export the data it had collected, categorising it as either energy or temperature measurements.

### Data Analysis MATLAB Program

The programs used to process and analyse the data acquired from the data logger were written in MATLAB. These programs were written individually for each experimental phase, with supplementary scripts that independently calculated parameters such as  $U_5$  and  $\dot{M}_5$ .

The program imported .csv files for the relevant runs [see Table 15 for key], formatted the data, and analysed it using embedded functions. Certain programs also outputted .m files which contained the independently calculated parameters used for other programs.

**Table 15:** Run number key for MATLAB program. Note that run numbers 10, 20, 30 were not used.

| Run number | Experimental Phase | $T_{sp}$ (° C) |
|------------|--------------------|----------------|
| 1 – 3      | 1                  | 160            |
| 4 – 6      | 1                  | 200            |
| 7 – 9      | 1                  | 240            |
| 11 – 13    | 2                  | 160            |
| 14 – 16    | 2                  | 200            |
| 17 – 19    | 2                  | 240            |
| 21 – 23    | 3                  | 160            |
| 24 – 26    | 3                  | 200            |
| 27 – 29    | 3                  | 240            |
| 31 – 33    | 4                  | 160            |
| 34 – 36    | 4                  | 200            |
| 37 – 39    | 4                  | 240            |

# **Safety Appendix**

Several actions were taken to minimise the risks and hazards in preparing and performing experiments for this research project.

## **Precautions During Setup**

The oven was partially disassembled to measure the thicknesses of the components of the wall. One of these components was insulation wool, which contains many fibres that can lead to skin irritation and so gloves were worn when performing these measurements.

If by chance an incident leads to excessive force being applied to any electrical cable in the system, this tension could disconnect the wiring at connection points and short circuit components if the system is running. To prevent this hazard, cable glands were used at connection points, including the box containing the power meters, as well as the mains connection at the back of the oven. This ensured that tension is dissipated around the connection points instead of at the connection points.

## **Precautions During Experiments**

Hazards derived from heat were the most significant source of danger during the runs; as a result, oven gloves were used to handle hot items such as the pseudo-chicken after the end of runs in Phases 3 and 4.

The highest temperatures the cooler unit and the water within would reach were  $\sim 30^{\circ}\text{C}$  during the time over which the experiments were performed. Although this was relatively cool and did not provide a hazard, the water reservoir within had the potential to leak and reach the electrical components at the back of the oven. This hazard was mitigated by elevating the cooler unit on a tray which also served as a container. Additionally, the water was allowed to drain out through a small hole made at the bottom of the cooler unit, without needing to detach the cooler unit from the oven or removing the nylon cover. To prevent flow out of the cooler unit during the runs, this hole was sealed off using a rubber bung.